LA-UR-17-23195 (Accepted Manuscript)

The application of visible absorption spectroscopy to the analysis of uranium in aqueous solutions

May, Iain; Colletti, Lisa Michelle; Copping, Roy; Garduno, Katherine; Lujan, Elmer J. W; Mauser, Ava Kerrigan; Meckler-Hickson, Alex; Reilly, Sean Douglas; Rios, Daniel; Rowley, John; Schroeder, Alex B.

To be published in: Talanta

DOI to publisher's version: 10.1016/j.talanta.2017.07.051

Permalink to record: http://permalink.lanl.gov/object/view?what=info:lanl-repo/lareport/LA-UR-17-23195

The application of visible absorption spectroscopy to the analysis of uranium in aqueous solutions

L.M. Colletti, R. Copping, K. Garduno, E.J.W. Lujan, A.K. Mauser, A. Mechler-Hickson, I. May, S.D. Reilly, D. Rios, J. Rowley, A.B. Schroeder

www.elsevier.com/locate/talanta

PII: S0039-9140(17)30773-7
DOI: http://dx.doi.org/10.1016/j.talanta.2017.07.051
Reference: TAL17750

To appear in: *Talanta*

Received date: 20 April 2017
Revised date: 14 July 2017
Accepted date: 17 July 2017

Cite this article as: L.M. Colletti, R. Copping, K. Garduno, E.J.W. Lujan, A.K Mauser, A. Mechler-Hickson, I. May, S.D. Reilly, D. Rios, J. Rowley and A.B. Schroeder, The application of visible absorption spectroscopy to the analysis o uranium in aqueous solutions, *Talanta* http://dx.doi.org/10.1016/j.talanta.2017.07.051

The application of visible absorption spectroscopy to the analysis of uranium in aqueous solutions

L.M. Colletti[a], R. Copping[a,b], K. Garduno[a], E.J.W. Lujan[a], A.K. Mauser[a,c], A. Mechler-Hickson[a,d], I. May[a,*], S.D. Reilly[a,*], D. Rios[a], J. Rowley[a] A.B. Schroeder[a,d]

[a]Los Alamos National Laboratory, P.O. Box 1663, Los Alamos, NM 87544, USA.

[b]Present address, Oak Ridge National Laboratory, P.O. Box 2008, Oak Ridge, TN 37831, USA.

[c]The University of New Mexico, Albuquerque, NM 87131, USA.

[d]The University of Wisconsin-Madison, Madison, WI 53715.

[*]Corresponding authors.

iainmay@lanl.gov

sreilly@lanl.gov.

Abstract

Through assay analysis into an excess of 1 M H_2SO_4 at fixed temperature a technique has been developed for uranium concentration analysis by visible absorption spectroscopy over an assay concentration range of 1.8 – 13.4 mgU/g. Once implemented for a particular spectrophotometer and set of spectroscopic cells this technique promises to provide more rapid results than a classical method such as Davies-Gray (DG) titration analysis. While not as accurate and precise as the DG method, a comparative analysis study reveals that the spectroscopic method can analyze for uranium in well characterized uranyl(VI) solution samples to within 0.3 % of the DG results. For unknown uranium solutions in which sample purity is less well defined agreement between the developed spectroscopic method and DG analysis is within 0.5 %. The technique can also be used to detect the presence of impurities that impact the colorimetric analysis, as confirmed through the analysis of ruthenium contamination. Finally, extending the technique to other assay solution, 1 M HNO_3, HCl and Na_2CO_3, has also been shown to be viable. Of the four aqueous media the carbonate solution yields the largest molar absorptivity value at the most intensely absorbing band, with the least impact of temperature.

Graphical Abstract

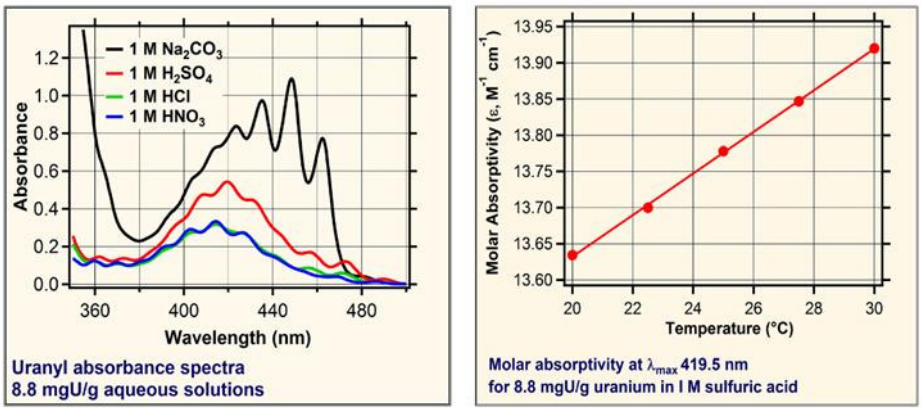

Keywords:

Uranium concentration analysis, Uranyl spectroscopy, Visible absorption spectroscopy

1. Introduction

The accurate and precise determination of uranium concentration in solution is essential for numerous applications, particularly within the multiple facets of the nuclear fuel cycle. Technological advances focus on uranium analysis in a wide range of matrices and actinide element concentrations. [1] The applications for uranium solutions also extends beyond conventional nuclear operations, with one pertinent example being the production of medical isotope Mo-99 from enriched uranium. Specifically, SHINE Medical Technologies are developing a Low Enriched Uranium (LEU) based process in which a deuterium tritium neutron generator would produce fission Mo-99 from a mildly acidic uranium sulfate target solution.[2] In such media uranium will be present in the +VI oxidation state as the uranyl dication (UO_2^{2+}). Through partnership with the National Nuclear Security Administration (NNSA) Office of Material Management and Minimization (M^3) research at both Argonne,[3] and Los Alamos,[4] National Laboratories have led to the development of separation processes for the recovery of Mo-99 from proposed SHINE target solutions. Research at Los Alamos has also been directed towards uranium concentration analysis in simulated SHINE process solutions. To meet Nuclear Regulatory Commission

Nuclear Material Accountancy requirements a tried and trusted method for uranium analysis, such as the Davies-Gray titration method, is required.[5-8] This method provides high precision and accuracy, but it is a time consuming process involving multiple analytical steps. To compliment this method we proposed the development of a relatively simple technique based on uranium absorption spectroscopy and the application of the Beer-Lambert law ($A = \varepsilon \cdot c \cdot l$, where $A =$ absorbance, $\varepsilon =$ molar absorptivity, $c =$ concentration, and $l =$ path length).

In most solution based applications uranium is present as the +VI uranyl dication (UO_2^{2+}). Uranyl(VI) complexes in solution typically have very distinctive absorption features in the visible spectrum region. Multiple vibronic bands are observed with energies and intensities that are highly dependent upon local symmetry, and hence thus the type and number of equatorial ligands (typically 4-6) coordinating the linear $\{O=U=O\}^{2+}$ moiety.[9-11] The observed absorption bands can be assigned based on current understanding of uranyl electronic structure, and associated molecular orbitals. Extensive work has been performed probing the uranyl moiety, with comprehensive summaries provided by Denning.[12-13] Briefly, excitations at > 30,000 cm^{-1} (< 330 nm) correspond to ligand to metal charge transfer (LMCT) transitions from the equatorial ligands (O_{eq}) to the uranium center (*i.e.* $LMCT_{eq}$). These transitions are dipole allowed and appear as a marked increase in the absorption coefficient with increasing energy, with no resolvable features. Moving towards the visible region (< 30,000 cm^{-1}, > 330 nm), transitions within the uranyl moiety occur from the highest occupied σ_u bonding orbitals, of $O_{ax}(2p)$ and U(5f) character, to the lowest unoccupied non-bonding uranium 5f orbitals (σ_u and δ_u). As these transitions originate from occupied molecular orbital with predominantly uranium *vs.* oxygen character, they can be considered as 5f-5f transitions. Such 5f-5f transitions are parity forbidden in centrosymmetric (D_{6h} & D_{4h}) systems by the Laporte selection rule, but gain intensity through local symmetry reduction and/or or coupling to vibrational modes. Vibronic coupling to the asymmetric uranyl modes (stretch, ν_2, and bend, ν_3) are the main source of transition intensity in a centrosymmetric environments (D_{4h}, D_{6h}).[14-16] Vibronic coupling to the symmetric O=U=O stretch (ν_1) occurs in both centrosymmetric and non-centrosymmetric complexes (D_{5h}, D_{3h}). Therefore, 5f-5f transitions with associated vibronic coupling results in the characteristic fine structure that are observed in most common uranyl absorption spectra. Clearly the strong influence of symmetry, and hence coordination environment, on uranyl(VI) spectroscopy makes it very advantageous to study well defined molecular systems in solution, allowing ε to be calculated at a fixed λ_{max}.

Recent advances in uranyl analysis by visible spectroscopy have focused on both nitrate and sulfate solution media, environments of relevance to many applications. Efforts have largely been directed towards analysis in different acid concentrations, and the deconvolution of spectral features attributed to

multiple species.[17-19] Our approach has been to develop a technique suitable for assay analysis, dilution of the sample in an excess of 1 M H_2SO_4. Through this procedure it was hypothesized that speciation could be kept constant, and hence ε and λ_{max} constant. It was postulated that maintaining constant ε and λ_{max} could increase technique accuracy and precision, simplify subsequent data analysis and increase the ease with which colored impurities could be identified. Finally, our previous development work has shown that fluctuating room temperature can impact the absorbance intensity at λ_{max}, hence molar absorptivity. This is not surprising as such temperature effects have previously been reported for uranyl spectra in aqueous media.[20-22]

We now report the development of a uranium concentration analysis technique by absorption spectroscopy at 22.5 °C in 1 M H_2SO_4, with contaminant impacts quantified and technique validation through comparison with Davies-Gray uranium concentration analysis. This study also includes an evaluation of extending the spectroscopic technique to uranium analysis in 1 M HCl, HNO_3 and Na_2CO_3 solutions through a study of the impact of temperature on molar absorptivity in these three media.

2. Experimental

2.1. Solution Preparations

1 M sulfuric acid solutions were prepared from 2.00 M (4.00 N) NIST traceable H_2SO_4 standard solutions through dilution with deionized H_2O. This was achieved through addition of 1.116-1.119 equivalents of 4 N H_2SO_4 to deionized H_2O, as measured accurately by mass. Bottle #1 1 M sulfuric acid was prepared using Fisher 4.00 (3.95 – 4.05) N standard solution (Lot ID 135119), bottles #2-4 were prepared using Fisher 4.00 (3.95-4.05) N standard solution (Lot ID 156253) and bottle 5 using LabChem 4.00 N H_2SO_4 (4.04 N, Lot ID E154-14). Using the density of H_2SO_4 as a function of wt % H_2SO_4 (International Critical Tables Data) the molarity of wt % H_2SO_4 solutions could be calculated at different temperatures.[23] This data could be used to determine the wt % H_2SO_4 in the different 4 N H_2SO_4 standard solution, where molarity data at a given temperature is provided (25 °C for the two Fisher solutions, and assumed to be the same for the LabChem solution.) This, in turn, allowed for the determination of wt % H_2SO_4 for bottles #1-5 – calculated to be 9.262, 9.262, 9.253, 9.253 & 9.284 % for bottles 1-5, respectively. Solution densities were measured at either 20.0, 27.5 and 35.0 °C (bottle #1) or 20.0, 25.0 and 30.0 °C (bottles 2-5), and the measured densities indicated that the Bottles #1-4 solutions were closer to 9.20 wt %, and thus 0.99 M at 25 °C. This value is within the uncertainty range of the original 3.95-4.05 N Fisher standard solution range. The bottle # 5 solution measured density data was slightly lower, closer to 9.10 wt % H_2SO_4 and thus 0.97 M at 25 °C. This may indicate that the original LabChem 4.00 N H_2SO_4 was not as

concentrated as expected. Throughout the rest of this work the conc. of H_2SO_4 in all five prepared H_2SO_4 solutions will simply be written as 1 M.

1.00 M HCl (RICCA, Lot ID 1600077) and 1.00 M HNO_3 (RICCA, Lot ID 2511516) were used as received and 1.0 M Na_2CO_3 was prepared by dissolution of anhydrous Na_2CO_3 (Fisher) in deionized H_2O. Throughout the rest of this work these solutions will all just be referred to as 1 M in concentration.

A uranium standard solution in nitric acid 100.00305(±0.00307) mg/g was prepared through dissolution of CRM 112-A uranium metal standard (New Brunswick Laboratory) in a known mass of nitric acid. Carefully weighed aliquots of this solution were transferred with deionized water into 9 separate 100 mL volumetric flasks. These volumetric flasks, with aluminum foil wrapped around the necks, were used to minimize any solution loss during heating to 300 °C, required to drive off nitric acid and nitrate. Once the samples were dry deionized water was added (*ca.* 10 mL) and the samples again heated to dryness. Lastly, deionized water was again added and the samples heated up to 400 °C for at least 45 min to ensure removal of all remaining nitrate and nitric acid as NOx gases, leaving orange solids of $UO_3{\cdot}{\times}H_2O$ at the bottom of each volumetric flask. Either bottle # 2 1 M H_2SO_4, 1 M HCl, 1 M HNO_3 or 1 M Na_2CO_3 were used to dissolve and wash out all of the uranium into pre-weighed HDPE sample bottles up to a pre-determined mass, thus generating standard solutions 1-9 (Table 1).

Samples 11-20 had unknown uranium concentrations and were used to test the uranium analysis technique developed from the molar absorptivity value calculated at 22.5 °C for solution 1-6. Each sample contained uranium in dilute sulfuric acid (pH range between 0.6-1.4). Samples 11, 12 & 20 were all natural uranium samples that had originated from CRM-112A standard material, while sample 14 was prepared from dissolution and acidification of $UO_2SO_4{\cdot}3H_2O$ (Biorad Industries). The remaining samples were prepared from depleted uranium sulfate stock solution and solids available in the laboratory. In each case *ca.* 1.4 mL of each samples were assayed into *ca.* 28 mL of either Bottle #4 or Bottle # 5 1 M H_2SO_4, with all manipulations recorded through accurate mass measurements. These assay solutions were analyzed by UV-vis absorption spectroscopy. Density measurements were recorded at 22.5 °C for the 1 M H_2SO_4 solutions, uranium samples and resultant uranium assay solutions.

10, 1.0 and 0.10 ppm ruthenium standard solutions in 1 M H_2SO_4 (Bottle #1) were prepared using GFS Ruthenium 10,000(±100) ppm ICP standard solution in 20 % HCl (NIST traceable, Lot ID C578362) through serial dilutions using bottle #1 1 M H_2SO_4. These solutions were analyzed by UV-vis spectroscopy on the day that they were prepared and 11 and 32 days later. Weighed 10 ml aliquots of Bottle #1 1 M H_2SO_4, and the 0.1, 1.0 & 10 ppm Ru solutions in 1 M H_2SO_4, were added to weighed 500 uL aliquots of a nominal 150 gU/L (129 mg/g) depleted uranium stock (pH 1.05) to yield samples 21-24,

respectively. The density of the 150 gU/L uranium stock solution was measured at 10.0, 15.0, 19.5, 20.0 and 25.0 °C, and the temperature dependent densities of the 0.1, 1.0 & 10 ppm Ru solutions assumed to be the same as previously measured for the bottle # 1 1 M H_2SO_4 used in their preparation.

2.2 Density Measurements

Density measurements were recorded on a Mettler Toledo DM50 density meter with integrated SC1 single sample automation. Each sample was measured at least in triplicate.

2.3 Spectroscopic Analysis

Spectroscopic measurements were performed using an Agilent Technologies Cary 60 Spectrophotometer with a Cary Peltier temperature control unit. Prior to recording spectra of any sample containing uranium at a set temperature, spectra were first collected on the corresponding 1 M aqueous solution (H_2SO_4, HCl, HNO_3 or Na_2CO_3) as a background measurement. In all cases spectra were recorded using two methods of data collection, the first being a conventional 'scan' measurement (600 nm – 300 nm range; with scan averaging time, data interval and scan rate of 0.1 s, 0.5 nm & 300 nm/min, respectively). While background corrected scan measurement data are reported in this work as representative figures this data was never used for quantitative analysis. The second set of recorded measurements were called 'reads' data measurements. Within the Agilent software a method was developed where absorbance data was averaged multiple times, but only at selected fixed wavelengths. Data was always collected at 600, 550 & 500 nm, the weighted average of the former two points used for baselne correction. For the uranyl(VI) spectra in each of the acid or base solutions data was also collected at λ_{max} and the two peaks adjacent to λ_{max}. For U(VI) in 1 M H_2SO_4 these transition were observed at 419.5, 409.0 & 430.0 nm, respectively. For each 'reads' measurement triplicate data sets were obtained.

Reads data for one uranium sample and the corresponding background matrix at a given temperature could be used to generate background and baseline corrected absorbance values. Firstly, the triplicate sample reads data at each wavelength were averaged, and the same task performed for the corresponding background matrix data. The background data was then subtracted from the sample data at each wavelength, resulting in background subtracted absorbance values at 409.0, 419.5, 430.0, 500.0, 550.0 & 600.0 nm in 1 M H_2SO_4, as an example. A weighted average of the 550 & 600 nm values was subtracted from the absorbance values at 409, 419.5, 430 & 500 nm to generate background and baseline subtracted absorbance values. The final λ_{max} value at 419.5 nm in 1 M H_2SO_4 would be used to either generate molar absorptivity, if the uranium concentration in solution was known in mg/g, or uranium concentration once the molar absorptivity value had been calculated. In the case of the [U] calculations, the assay dilution had to be incorporated to provide the uranium conc. (mg/g) of the actual sample as samples would be

prepared through dilution into 1 M H_2SO_4. By taking ratios of the 409.5 nm value with the absorbance values at 419.5, 430.0 & 500.0 nm any deviation in said ratios could be probed, indicative of issues with the measurement and/or the presence of impurities. Comparison of background corrected 550 & 600 nm absorbance values could also be used for the same purpose. Finally, for each spectroscopic measurement three different Starna 10.00(±0.01) nm quartz UV-vis cells were used, with background matrix measurements linked to the same cell. Thus all absorption spectroscopy measurements reported in this work have been made in triplicated in three different cells.

The Agilent temperature control unit was calibrated using a UV-vis cell filled with deionized water and a matching pair of external temperature probes attached to a FLUKE 54IIB thermometer. Across the 5 different temperature settings used in this study (20.0, 22.5, 25.0, 27.5 & 30.0 °C) both the difference between the Peltier unit temperature and UV-vis solution cell temperature, and the time taken for the solution temperature to reach equilibrium with the Peltier unit temperature, were monitored. Typically the solution temperature would be in good agreement the the Peltier unit temperature (± 0.1 °C), and after changing temperature on the Peltier unit the corresponding solution temperature would typically match within minutes. Despite the efficiency of the Peltier unit, laboratory temperature would on occasion impact the time taken for the unit to reach a new temperature setting and thus additional time would often be allowed for the solution temperature to equilibrate during actual measurements.

The ruthenium contaminant analysis work was performed prior to the use of Peltier temperature control unit and for these experiments the room temperature was recorded at the time of measurement. For samples 21-24 the uranium concentration was measured using previously calculated temperature dependent molar absorptivity values for uranium in 1 M H_2SO_4; Starna cell 1 = 13.368+(0.019×T), cell 2 = 13.450+(0.017×T) & cell 3 = 13.443+(0.017×T) (where T = measurement temp in °C). Typical 1σ uncertainties associated with these ε values were 0.4 %, while on occasions accurate temperature measurements were not recorded and for some samples the measurement temperature was outside the density measurement range of the original uranium stock solution. In practical terms we believe that the higher uncertainties associated with ε was the dominant contributor to uncertainty, and uncertainties associated with the other two factors were not quantified.

2.4. Davies-Gray Analysis

Aliquots of unknown samples 11-20 were taken for uranium analysis by the modified Davies-Gray method. As the Davies-Gray analysis was undertaken a few weeks after the spectroscopic analysis there may be a slight systematic bias due to factors such as sample evaporation or moisture absorption. Sample solutions were directly transferred into individual tared 30 mL PPE dropper bottles. Weights for

transferred solutions were recorded, but no attempt was made to perform a quantitative transfer as the desired assay was for the uranium concentration of the solution and not the total amount of uranium within the original container. Samples were diluted to approximately 30 grams with reagent grade 0.5 M H_2SO_4 and a final weight was taken. Bottles were shaken well to mix the solution. For each sample, two portions of accurately weighed 1.5 g samples, were aliquoted for analyses into 100 mL Pyrex beakers. Uranium assay was performed using a modified Davies-Gray titration method with cerium sulfate as the titrant. This method is very similar to ISO 7097-2 [24]. This method is statistically equivalent to using potassium dichromate as the titrant [25].

3. Results and Discussions

3.1. Molar absorptivity as a function of temperature in various aqueous media

The impact of calibration standards, spectroscopic data collection method and sample assay into an excess of a known aqueous medium have all previously been investigated in the course of our development of a visible spectroscopy uranium analysis method for uranyl solutions assayed into 1 M H_2SO_4.[26] However, uranyl absorption spectroscopic features are known to be influenced by temperature, and thus technique accuracy and precision can be impacted if solution temperature is not controlled. While the main focus of this study was on developing an assay method in 1 M H_2SO_4 the impact of temperature on uranyl ε and λ_{max} were also studied in different aqueous media for comparison. Natural uranium standard solutions of 8.8 mg/g concentration were prepared in 1 M H_2SO_4, HCl, HNO_3 & Na_2CO_3 (samples 4, 7, 8 & 9, respectively), as shown in Table 1. Absorption spectra related to this study are shown in Figures 1 & 2. Temperature dependent calculated molar absorptivity data at λ_{max} for uranyl in each of the different solution matrices are given in Table 2, with the data derived using Equations 1.

The spectra of uranyl in 1 M HCl and 1 M HNO_3 share very similar features, with ε and λ_{max} values close to what would be observed for D_{5h} $UO_2(OH_2)_5^{2+}$ in perchlorate solutions.[27-29] In 1 M HCl the slight increase in molar absorptivity vs. $UO_2(OH_2)_5^{2+}$ can be ascribed to the presence of a second species, UO_2Cl^+ (aq),[30-31] with the somewhat broadened transitions almost identical to those previously observed in 1 M Cl^- solution.[29] In a comparable situation the slight increase in molar absorptivity for λ_{max} in 1 M HNO_3 vs. $UO_2(OH_2)_5^{2+}$ is due to the presence of another second species, $UO_2(NO_3)^+$.[17, 22, 32]

Recent visible spectroscopy studies for uranyl in sulfate media have focused on pH range solutions, rather than 1 M H_2SO_4, and on solution speciation rather than uranium concentration measurement.[18-19, 33]

Nevertheless, the reported spectral features attributed to UO_2SO_4 (aq), with a λ_{max} of *ca.* 420 nm,[18, 33] are very similar to the 419.5 nm λ_{max} observed in these 1 M H_2SO_4 studies. The reported molar absorptivity value for UO_2SO_4 (aq) (between 13-14 M^{-1} cm^{-1}) is also consistent with the values obtained in this study in 1 M H_2SO_4.[33] It would thus appear that UO_2SO_4 (aq) is the predominant uranyl chemical species in 1 M H_2SO_4.

In 1 M Na_2CO_3 $UO_2(CO_3)_3^{4-}$ dominates speciation, and the 6 coordinate D_{3h} complex has higher symmetry than observed for the chemical species in 1 M H_2SO_4, HCl or HNO_3. This results in very distinctive spectroscopic feature, with four comparatively lower energy peaks dominating the spectroscopic signature, as previously observed for both $UO_2(CO_3)_3^{4-}$ and $UO_2(NO_3)_3^{-}$ in different solution environments.[34-38] In this study at 22.5 °C the molar absorptivity for U(VI) in 1 M Na_2CO_3 was calculated to be 26.479(±0.0030), 26.481(±0.0032) and 26.498(±0.030) M^{-1} cm^{-1} when recorded in the three Starna cells (Table 2) at λ_{max} 448.5 nm. This is in good agreement with a reported value of ε = 26.3(±0.3) M^{-1} cm^{-1} at λ_{max} 448.5 nm reported for $UO_2(CO_3)_3^{4-}$ in 0.5 M Na_2CO_3.[34]

The impact of temperature between 20 - 30 °C on the uranyl(VI) λ_{max} peak in all four 1 M ionic media (H_2SO_4, HCl, HNO_3 & Na_2CO_3) are shown in Figures 2 & 3, with molar absorptivity data provided in Table 2. Figure 2 clearly shows that there is an increase in peak intensity in all four solutions as a function of temperature, in line with previous studies.[20-22] Only in 1 M HNO_3 is there a significant shift in λ_{max} over this temperature range. Figure 3 and Table 2 show good agreement between calculated molar absorptivity's for all three Starna cells at each measured temperature. Also, the impact of temperature on molar absorptivity increases across the series Na_2CO_3 < HNO_3 < HCl < H_2SO_4. This may reflect the fact that uranyl speciation is unlikely to vary greatly in carbonate solution, but additional nitrate, chloride and sulfate complexation as the temperature is increased is likely in the other solution environments. Of most relevance to the remainder of this study is the significant impact of temperature on the molar absorptivity at λ_{max} in 1 M H_2SO_4, which increases by 0.4 % every 1 °C increase in temperature. The development of a spectroscopic uranium analysis technique in this medium requires careful temperature control if temperature derived uncertainties are to be minimized.

The data work up for the reads measurements used to determine the variable temperature molar absorptivity values highlighted the importance of high quality background solution measurements. Initial analysis of uranyl(VI) in1 M HCl data revealed significantly lower ε for cell 1 vs. cells 2 & 3. This could be attributed to higher recorded triplicate 1 M HCl baseline reads for cell one at all temperatures. These measurements were subsequently re-recorded and found to be more in line with values already obtained for cells 2 & 3. For 1 M Na_2CO_3 at 30.0 °C the cell 3 molar absorptivity value is significantly greater, and

with increased associated uncertainties, than recorded in cells 1 & 2. This could be attributed to higher recorded baseline reads values in this cell for one of the triplicate measurements. Unfortunately a repeat measurement was not possible.

3.2. Determination of the Molar Absorptivity of Uranium in 1 Molar Sulfuric Acid at 22.5 ℃ as a function of uranium concentration

Samples 1-6 contained various concentrations of uranium (mg/g) in 1 M H_2SO_4 (Table 1), with the spectra of all 6 samples presented in Figure 4 clearly showing the expected increase in spectra intensity as a function of uranium concentration. Molar absorptivity values at λ_{max} 419.5 nm were calculated at each uranium concentration, Table 3 and Equation 1. Repeat data measurements were made for samples 1 & 3. The uncertainties for the molar absorptivity values were lower for two out of the three cells for the sample 1 repeat measurements, while the sample 3 repeat measurements yielded molar absorptivity values within the margin of error (1σ) of the original sample 3 measurements. In both cases the repeat measurements are included here.

While Table 3 reports molar absorptivity's for uranyl at λ_{max} in 1 M H_2SO_4 at the different uranium concentrations, for application in uranium concentration analysis single molar absorptivity values were required across the [U] for each Starna cell. These values were calculated for Starna cells 1-3 using the data in Table 4, which was in turn incorporated into the plots presented in Figures 5 & 6. Firstly, plots of absorbance vs. uranium conc. for all three Starna cells yielded linear fits which could be extrapolated essentially to zero for both variables, as expected for adherence to Beer Law. Secondly, plots of absorbance vs. cell path length × uranium conc. were fitted with straight lines where the y intercept was fixed at zero (Figure 6). This second plot yielded Beer-Lambert fits where the slope of the line was equivalent to the molar absorptivity across the measured uranium concentration range. For all three Starna cells 10.00(±0.01) mm these fits were weighted with the 1σ uncertainty in the values from both axis, yielding molar absorptivity values for uranyl(VI) in 1 M H_2SO_4 at 22.5(±0.1) °C of 13.716(±0.006) cell 1, 13.715(±0.006) cell 2 & 13.724(±0.006) cell 3. It is these molar absorptivity values that were used to calculate uranium concentration from measured absorbance values at 419.5 nm for unknown solutions 11-20.

Samples 1-6 were not only used to determine ε from λ_{max} at 419.5 nm, but were also be used to determine the ratio of the 419.5 nm peak to the 409 & 430 nm peaks for these standard solutions. The ratio of the 419.5 nm peak to the absorbance at 500 nm and the weighted average absorbance at 550 & 600 nm (baseline correction value) were also plotted. This absorbance value data is presented in Figure 7 for solutions 1-6 in Starna cells 1-3, and will be used as the 'expected' values for pure U(VI) in 1 M H_2SO_4

solutions. This data will be revisited in later discussion when probing if solution contaminants or impurities invalidate subsequent uranium concentration analysis measurements.

3.3. Determination of uranium concentration in uranium sulfate solutions by both the visible spectroscopy method and by Davies-Gray titration analysis

With molar absorptivity values determined for uranium in 1 M H_2SO_4 at 419.5 nm (22.5 °C) it was now possible to calculate uranium concentrations for unknown samples spectroscopically, if they were diluted into excess 1 M H_2SO_4 and measurements performed at 22.5 °C using the appropriate 1 cm path length Starna cells. 10 unknown samples in dilute sulfuric acid (samples 11-20) were thus analyzed by visible spectroscopy, after first assaying into an excess 1 M H_2SO_4. Uranium concentrations (mg/g) were calculated using both the density of the unknown samples and the density of the original 1 M H_2SO_4 assay acid at 22.5 °C, and also the density of the unknown sample and the density of the actual assay solution at 22.5 °C. The results obtained from both calculations were identical within 1σ and only the uranium concentrations calculated using the density of the unknown sample and the density of the original 1 M H_2SO_4 assay acid at 22.5 °C are reported here (Equations 2 & 3).

Samples 11-20 were also subsequently analyzed for uranium concentration using the standard Davies-Gray titration method. Uranium titration analysis can be undertaken under a large variety of conditions using many different reagents; however, the most commonly used and accepted technique is based on a method developed by Davies and Gray in 1964 [5]. This method can determine precise uranium assay values with minimum interferences and without requiring separations prior to the assay of uranium materials. The uranium is reduced to U(IV) by excess Fe(II) in strong phosphoric-sulfamic acid, and excess Fe(II) is selectively oxidized by nitric acid in the presence of a Mo(VI) catalyst. Then the U(IV) can be titrated either with a dichromate solution or with a cerium sulfate solution, with a potentiometric titration using vanadyl as electrochemical enhancer.

The Davies-Gray titration method used for uranium assay has been reviewed and improved by many authors since its first introduction [8. 24-25, 39-40]. Experience with titrations indicates either automated or manual titrations can be performed equally well, the choice of which determined by the frequency of the analysis and other factors [25]. The uranium assay measurements for this study were performed using a modified Davies-Gray titration method with cerium sulfate as the titrant. This method is very similar to ISO 7097-2 [24], and statistically equivalent to using potassium dichromate as the titrant [25]. The biggest difference between the potassium dichromate and cerium sulfate titrations has been the sharpness of the end point, with the cerium sulfate having a sharper endpoint. Care was taken not to over titrate while using cerium sulfate as the titrant.

The results of both sets of uranium concentration analysis are presented in Table 5, and in Figures 8-10. Absorbance value comparisons for the assay analysis of samples 11-20 are also presented in Figure 11.

For unknown samples 11-20 the uranium analysis results by the visible spectroscopy technique were in excellent agreement for cells 1, 2 & 3, with one exception - the cell 1 analysis of sample 18 assayed into LabChem 1 M H_2SO_4 (Table 5 & Figure 10). The calculated uranium concentration is significantly higher for this one measurements than for the other 5 sample 18 spectroscopic analyses – cells 2 & 3 analysis using LabChem 1 M H_2SO_4 assay and cells 1-3 analyses assayed using Fisher 1 M H_2SO_4. In addition, the calculated uncertainties associated with this measurement are greater than for the other sample 18 spectroscopic method analyses. Finally, the uncertainties associated with the 419.5/409 nm and 419.5/430 nm peak ratios are greater than for the other sample 18 measurements, the 419.5 nm/500nm ratio lower and the ave. abs 550/600 nm higher (Figure 11). This can all be traced back to elevated reads absorbance values for both the background and samples measurements in this particular cell for this specific sample, and would justify discarding this data. Nevertheless, the remaining two cell measurements using LabChem 1 M H_2SO_4 assay acid were in good agreement with the three cell measurements using the Fisher 1 M H_2SO_4, indicating that the technique is rigorous to change in acid supplier.

Turning to the comparison between the Davies-Gray analysis and the visible spectroscopy analysis, samples 11, 12 & 20 were prepared from a different batch of the same standard reference material as used to prepare all the molar absorptivity measurement standards (CRM 112-A). In addition, sample 14 was prepared from uranyl sulfate trihydrate purchased from Biorad industries. All four of these samples had a well-known chemical history, with no introduction of potential contaminants, and the spectroscopic results were in good agreement with the Davies-Gray measurements (Table 5 and Figure 8). This indicates that with uranium samples of known purity the developed visible spectroscopy technique will provide [U] within the *ca.* 0.3 % expanded uncertainties associated with the measurements.

The remaining 6 unknown samples were prepared from depleted uranium stocks where there was no direct knowledge of the presence or absence of potential contaminants (colored or suspended particulates). These samples would prove to be a useful test of the impact of potential impurities on the visible spectroscopy uranium analysis measurement. For samples 16 and 17 again there was very good agreement between the visible spectroscopy and Davies Gray measurements, whereas for sample 13 and 15 the average difference between the two techniques was slightly higher (*ca.* 0.5 % on average), and thus slightly outside the reported uncertainties (Figure 9). For almost all of the samples discussed thus far the Davies-Gray results produced uranium concentration results slightly higher than the visible spectroscopy

measurements. This could, in part, be attributed to sample evaporation that occurred between spectroscopic and Davies-Gray analyses (Table 5 and Figures 8 & 9). The exception to this systematic bias was the sample 17 analysis where the spectroscopic method yielded slightly higher uranium concentration results than the Davies-Gray method. This discrepancy could attributed to an impurity in the sample, as evidenced by the significantly lower sample 17 419.5/409 and 419.5/500 nm peak ratios than observed for samples 1-6 and the significantly higher average sample 17 550 & 600 nm absorbance value than previously observed for samples 1-6 (Figure 11).

Even when discounting the anomalously high uranium concentration analysis for 1 of the 6 sample 18 spectroscopic measurements (as previously discussed) the other 5 spectroscopic analyses yielded significantly higher uranium concentration results than the corresponding Davies-Gray analyses for this unknown sample (Table 5, Figure 10). In a comparable situation to sample 17, the presence of an impurity is indicated by the absorbance value comparisons for the sample 18 measurements vs. those previously observed for samples 1-6 (Figure 11).

In summary, analysis of 7 of the 9 unknown samples yielded spectroscopic and Davies-Gray results that were in good agreement. These analysis appeared to validate the calculated uncertainties for the spectroscopic method, except for the lower concentration bias vs. the Davies-Gray method. For the other 2 unknown samples a comparison of absorbance values indicates the presence of impurities which could have impacted, and hence invalidated, the results.

The uranium concentration analysis results obtained for sample 19 were on average almost 3 % higher by the spectroscopic method than by the Davies-Gray measurement technique (Figure 10). This was a much larger than expected difference and there was no evidence in either the absorbance metrics (Figure 11) or reanalysis of the raw data for any contaminants or measurement errors. While this was the most concentrated sample the absorbance at 419.5 nm of the assay solution was comfortably within the technique molar absorptivity calibration range (Table 1, absorbance value range). The most likely cause of at least some of this discrepancy was mass measurement errors during sample preparation, but unfortunately this particular unknown samples was completely consumed in the initial analysis and thus further investigation was not possible.

3.4. Impact of Ruthenium Species on Spectroscopic Analysis of Uranium

Spectroscopic analysis related to the 409, 430, 500, 550 & 600 nm absorbance values appeared to be effective in highlighting the impact of undetermined and unquantified impurities in unknown samples 17 & 18. A more quantitative assessment of this impurity detection methodology was also undertaken through addition of a known impurity to uranium spectroscopic samples. As SHINE Medical

Technologies are striving to produce fission product Mo-99 from LEU uranyl sulfate solutions efforts were focused on fission product elements. An initial screen indicated that ruthenium species were by far the most intensely colored and thus the impact of ruthenium on the uranium absorption spectroscopy method was investigated.[41]

Serial dilutions of 10,000 ppm Ru standard solution in HCl into 1 M H_2SO_4 yielded 10, 1.0 and 0.1 ppm Ru solutions. In all solutions their spectral features were near identical, except for the expected order of magnitude decrease in absorbance across the 10>1.0>0.1 ppm series. However, these spectral features changed markedly 11 days after preparation, with negligible additional changes after 32 days. Figure 12 shows the absorption spectra of the 10 ppm solution after initial preparation and 32 days later. The initial spectra has a λ_{max} of 460 nm with an observed molar absorptivity of *ca.* 4000 M^{-1} cm^{-1}, which is similar to $Ru(IV)Cl_6^{2-}$ in chloride solution (λ_{max} = 480 nm, ε = 4800 M^{-1} cm^{-1}), presumably the dominant species in the 20 % HCl standard solution.[42] Over time the peak intensity diminishes by an order of magnitude to yield spectra which much more closely resemble Ru(IV) in sulfuric acid.[43]

Weighed 0.5 mL samples of a 129 mg/g uranium solution in pH 1 sulfuric acid were added to weighed 10 mL samples of 1 M H_2SO_4 (samples 21), 0.1 ppm Ru in 1 M H_2SO_4 (sample 22), 1.0 ppm Ru in 1 M H_2SO_4 (sample 23) and 10 ppm Ru in 1 M H_2SO_4 (sample 24). This is the equivalent to a nominal 0, 2.1, 21 & 210 ppm ruthenium concentration in the original 129 mg/g uranium solution for samples 21-24, respectively. The regular scan absorption spectra on day 1 clearly show the impact of a nominal 210 ppm Ru contaminant on the uranyl spectrum, and also show the impact of 21 ppm Ru contaminant (Figure 13). As observed for the Ru spectra in 1 M H_2SO_4, Ru speciation changes as a function of time alter the impact of Ru contaminant on the uranyl spectral features. Figure 13 shows the decreased impact of a 210 ppm Ru contaminant on the assay spectra of 129 mg/g uranium as a function of time.

Spectroscopic uranium concentration analysis was performed on solutions 21-24 on the day the solutions were prepared (day 1) and days 31 & 51. Table 6 contains the 'observed' uranium concentration results, with Figures 14-17 showing the analysis of the reads absorption values. The experimental method described for the spectroscopic measurements of samples 1-9 and 11-20 was not completely matched for samples 21-24. The most obvious difference was the lack of rigorous temperature control during the sample 21-24 measurements, which most significantly impacted the molar absorptivity values, and associated uncertainties, used for λ_{max} at 419.5 nm. Nevertheless, for all measurements there was good agreement between the uranium concentrations for sample 21, no ruthenium. In addition, apart from one elevated average 550 & 600 nm absorbance value (day 31, cell 2), all the absorbance value analysis was in good agreement with the sample 1-6 measurements (Figure 14). This consistent sample 21 'control' data gave confidence that the measurement results obtained for samples 22-24 would provide a good

assessment of the impact of Ru contaminant. For sample 22 the uranium concentration was the same within uncertainties across days 1, 31 & 51 as observed for sample 21. In addition, the analysis of absorbance values yielded data within the range of samples 1-6 (Figure 15). It could thus be included that a nominal 2.1 ppm Ru contaminant in a 129 mg/g uranium solution has no impact on uranium concentration analysis by the developed visible spectroscopy technique, at these uncertainty levels.

The day 1 'observed' uranium concentration spectroscopic measurements for samples 23 (nominal 21 ppm Ru contaminant) were significantly higher than observed for samples 21 & 22, but were the same within uncertainties with these two samples for days 31 & 51. If the analysis of absorbance values was to be of value then it should provide evidence for the presence of contaminant for the day 1 samples 23 measurement, indicating an invalid measurement. Looking at Figure 16 this is indeed the case with both the ratios of the 419.5/409 nm and the 419.4/500 nm absorbance's being significantly lower than observed for samples 1-6 on day 1 only. Finally, the 210 ppm Ru contaminant analysis (sample 24) resulted in 'observed' uranium concentration measurements significantly higher than 129 mg/g for all 3 time measurements and all four absorbance value analysis metrics were significantly outside of the range for samples 1-6 (Figure 17).

In summary, the Ru contaminant study provided evidence that analysis of the 409, 430 and 500 nm absorbance values, along with λ_{max} 419.5 nm and the baseline peaks at 550 & 600 nm, could determine when an absorbing contaminant impacts the spectroscopic uranium concentration analysis technique. This yields increased confidence that our assessment that the analysis of samples 17 & 18 were compromised by unknown contaminants is valid. The four samples (21-24) analyzed on 3 different time periods yielded 4 artificially high observed uranium concentration values. In each case analysis of absorbance values indicated that there was an issue with the measurement. Interestingly, the ratios of 419.5/409 and 419.5/500 nm absorbance values and the average of the 550 & 600 nm absorbance values appear more sensitive to the impact of impurities in samples 23 & 24, and indeed samples 17 & 18, when compared to the 419.5/430 nm ratio.

4. Conclusions

A uranium assay analysis technique has been developed, based on a calculated molar absorptivity at λ_{max} for the visible spectroscopy of the uranyl(VI) cation in 1 M H_2SO_4 at 22.5 °C. Through comparison with Davies-Gray titration analysis, the technique can be used to determine uranium concentration to within 0.3 % for high purity uranium samples in dilute sulfuric acid, and to within 0.5 % where the purity is less well defined. Solution impurities that impact the measurement method can be monitored, as evidenced through the analysis of ruthenium contaminated samples. Finally, we have shown that the assay technique

can be extended to other media, 1 M HNO_3, HCl and Na_2CO_3, with the molar absorptivity of λ_{max} for U(VI) in 1 M Na_2CO_3 least impacted by temperature.

Acknowledgements

We thank the National Nuclear Security Administration (NNSA) Office of Material Management and Minimization (M^3) for funding and J. Driscoll (SHINE) for useful discussions. We also thank the Los Alamos National Laboratory Seaborg Institute for a Summer Research Fellowship (A. B. Schroeder) and the University of New Mexico Science, Technology, Engineering, and Mathematics Talent Expansion Program funded through the National Science Foundation for a summer fellowship (A.K. Mauser).

References:

[1] D.P.S Rathore, Advances in technologies for the measurement of uranium in diverse matrices. Talanta 77 (2008) 9-20.

[2] K. Pitas, G. Piefer, SHINE technology and progress towards US-based molybdenum-99 production, J. Nucl. Med. 56 (2015) 165.

[3] L. Ling, P.L. Chung, A. Youker, D.C. Stepinski, G.F. Vandegrift, N.H.L. Wang, Capture chromatography for Mo-99 recovery from uranyl sulfate solutions: minimum-column-volume-design method., J. Chromatogr. A. 1309 (2013) 1-14. A. Youker, S.D. Chemerisov, M. Kalensky, P. Tkac, D.L. Bowers, G.F. Vandegrift, A solution-based approach for Mo-99 production: considerations for nitrate versus sulfate media. Science and Technology of Nuclear Installations (2013) 402570, **10 pages**.

[4] G.E. Dale, D.A. Dalmas, M.J. Gallegos, K.R. Jackman, C.T. Kelsey, I. May, S.D. Reilly, G.M. Stange, Mo-99 separation from high-concentration irradiated uranium nitrate and uranium sulfate solutions. Ind. Eng. Chem. Res. 51 (2012) 13319-13322.

[5] W. Davies, W. Gray, A rapid and specific titrimetric method for the precise determination of uranium using iron(II) sulphate as reductant. Talanta 11 (1964) 1203-1211.

[6] K.J. Mathew, S. Bürger, S. Vogt, P. Mason, M.E. Morales-Arteaga, U.I. Narayanan, Uranium assay determination using Davies and Gray titration: an overview and implementation of GUM for uncertainty evaluation. J. Radioanal. Nucl. Chem. 282 (2009) 939-944.

[7] P. Sahoo, C. Mallika, R. Ananthanarayanan, F. Lawrence, N. Murali, U. Kamachi Mudali, Potentiometric titration in a low volume of solution for rapid assay of uranium: application to quantitative electro-reduction of uranium(VI). J. Radioanal. Nucl. Chem. 292 (2012) 1401-1409.

[8] M. Bickel, The Davies-Gray titration for the assay of uranium in nuclear materials: a performance study. J. Nucl. Mater. 246 (1997) 30-36.

[9] C. Görller-Walrand, S. De Jaegere, Comparative study on absorption-spectra of uranyl complexes in solution and solid-state – symmetrical complexes C_S, $D_{2H}(6)$ and $D_{3H}(6)$. Journal de Chimie Physique et de Physico-Chimie Biologique 1972, 726-**736**.

[10] C. Görller-Walrand, S. De Jaegere, Comparative study of uranyl halide absorption-spectra – complexes with $D_{2H}(4)$ and $D_{3H}(3)$ $D_{4H}(4)$ and $D_{5H}(5)$ symmetry. Journal de Chimie Physique et de Physico-Chimie Biologique 1973, 70, 360-366.

[11] S.F. Lincoln, A. Ekstrom, G.J. Honan, Equatorial ligand effects on the visible spectra of dioxouranium(VI) complexes in solution. Australian Journal of Chemistry 35 (1982) 2385-2391.

[12] R.G. Denning, Electronic structure and bonding in actinyl ions and their analogs. J. Phys. Chem. 111 (2007) 4125-4143.

[13] R.G. Denning, Electronic structure and bonding in actinyl ions. Structure and Bonding 79 (1992) 215-276.

[14] P. Nockemann, K. Servaes, R. Van Deun, K. Van Hecke, L. Van Meervelt, K. Binnemans, C. Görller-Walrand, Speciation of uranyl complexes in ionic liquids by optical spectrscopy. Inorganic Chemistry **(2007)**, 46, 11335-11344.

[15] K. Servaes, C. Hennig, I. Billard, C. Gaillard, K. Binnemans, C. Görller-Walrand, R. Van Deun, R. Speciation of uranyl nitrato complexes in acetonitrile and in the ionic liquid 1-butyl-3-methylimidazolium bis(trifluoromethylsulfonyl)imide. European Journal of Inorganic Chemistry (2007)**, 2007,** 5120-5126.

[16] C. Hennig, K. Servaes, P. Nockemann, K. Van Hecke, L. Van Meervelt, J. Wouters, L. Fluyt, C. Görller-Walrand, R. Van Deun, Species distribution and coordination of uranyl complexes in acetonitrile. Inorganic Chemistry 47 (2008) 2987-2993.

[17] N.A. Smith, G.S. Cerefice, K. R. Czerwinski, Fluorescence and absorbance spectroscopy of the uranyl ion in nitric acid for process monitoring applications. J. Radioanal. Nucl. Chem. 295 (2013) 1553-1560.

[18] G. Meinrath, S. Lis, Z. Piskula, Z. Glatty, An application of the total measurement uncertainty budget concept to the thermodynamic data of uranyl(VI) complexation by sulfate. J. Chem. Thermodynamics, 38 (2006) 1274-1284.

[19] D. Vopálka, K. Štamberg, A. Motl, The Study of the speciation of uranyl-sulphate complexes by UV-Vis absorption spectra decomposition, J. Radioanal. Nucl. Chem. 286 (2010) 681-686.

[20] G. Götz, G. Geipel, G. Bernhard, The influence of the temperature on the carbonate complexation of uranium(VI): a spectroscopic study, J. Radioanal. Nucl. Chem. 287 (2011) 961-969.

[21] O.M. Suleimenov, T.M. Seward, J.K. Hovey, A spectrophotometric study on uranyl nitrate complexation to 150 °C, J. Solution Chem. 36 (2007), 1093-1102.

[22] L. Rao, G. Tian, Thermodynamic study of the complexation of uranium(VI) with nitrate at variable temperatures, J. Chem. Thermodynamics 40 (2008) 1001-1006.

[23] E.W. Washburn (Ed.), International Critical Tables of Numerical Data, Physics Chemistry and Technology (Knovel) **(2003)**.

[24] ISO 7097-2. Nuclear fuel technology - Determination of uranium in solutions, uranium hexafluoride and solids Part 2: Iron(II) reduction/cerium(IV) oxidation titrimetric method (2004).

[25] G. J. Slanina, F. Bakker, A.J.P. Groen, W.A. Lingerak, Accurate and precise determination of 2-25 mg amounts of uranium by means of a special automated potentiometric titration. Fresenius Z. Anal. Chem., 289 (1978) 102-105.

[26] I. May, S.D. Reilly, R. Copping, D. Rios, Uranium measurement control and total uranium concentration determination, Los Alamos National Laboratory, **(2014)** LA-UR-14-25139.

[27] J.T. Bell, R.E. Biggers, The absorption spectrum of the uranyl ion in perchlorate media, J. Molecular Spectroscopy 18 (1965) 247-275.

[28] K. Servaes, C. Hennig, I. Billard, C. Gaillard, K. Binnemans, C. Görller-Walrand, R. Van Deun, Speciation of uranyl nitrato complexes in acetonitrile and in the ionic liquid 1-butyl-3-methylimidazolium bis(trifluoromethylsulfonyl)imide, Eur. J. Inorg. Chem. (2008) 5120-5126.

[29] R.M. Rush, J.S. Johnson, Hydrolysis of uranium(VI): absorption spectra of chloride and perchlorate solutions, J. Phys. Chem. 67 (1963) 821-825.

[30] W. Runde, M.P. Neu, S.D. Reilly, Actinyl(VI) carbonates in concentrated sodium chloride solutions: characterization, solubility and stability, in D.T. Reed, S.B. Clark, L. Rao (Eds.) Actinide Speciation in High Ionic Strength Media, Springer, 8 (1999) 141-151.

[31] W. Runde, M.P. Neu, S.D. Conradson, D.L. Clark, P.D. Palmer, S.D. Reilly, B.L. Scott, C.D. Tait, Spectroscopic investigation of actinide speciation in concentrated chloride solution, Mat. Res. Soc. Symp. Proc. 455 (1997) 693-703.

[32] N.A. Smith, K.R. Czerwinski, Speciation of the uranyl nitrate system via spectrophotometric titrations, J. Radioanal. Nucl. Chem. 298 (2013) 1777-1783.

[33] C. Hennig, A. Ikeda, K. Schmeide, V. Brendler, H. Moll, S. Tsushima, A.C. Scheinost, S. Skanthakamur, R. Wilson, L. Soderholm, K. Servaes, C. Görrler-Walrand, R. Van Deun, Radiochim. Acta 96 (2008) 607-611.

[34] G.S. Goff, L.F. Brodnax, M.R. Cisneros, S.M. Peper, S.E. Field, B.L. Scott, W.H. Runde, First Identification and Thermodynamic Characterization of the Ternary U(VI) Species, $UO_2(O_2)(CO_3)_2^{4-}$, in UO_2-H_2O_2-K_2CO_3 Solutions, Inorg. Chem. 47 (2008) 1984-1990.

[35] T. Watanabe, Y. Ikeda, A Study on Identification of uranyl Complexes in Aqueous Solutions Containing Carbonate Ion and Hydrogen Peroxide, Energy Procedia, 39 (2013) 81-95.

[36] L. Stassen, J. Suthiram, Initial development of an alkaline process for recovery of uranium from ^{99}Mo production process waste residue, J. Radioanal. Nucl. Chem. 305 (2015) 41-50.

[37] A. Ikeda, C. Hennig, S. Tsushima, K. Takao, Y. Ikeda, A.C. Scheinost, G. Bernhard, Comparative Study of Uranyl(VI) and –(V) Carbonato Complexes in an Aqueous Solution, Inorg. Chem. 46 (2007) 42**12**-4219.

[38] P. Nockemann, K. Servaes, R. Van Deun, K. Van Heck, L. Van Meervelt, K. Binnemans, C. Gŏrller-Walrand, Speciation of Uranyl Complexes in Ionic Liquids by Optical Spectroscopy. Inorg. Chem.. **46 (2007), 11335-11344.**

[39] K.J. Mathew, S. B**ū**rger, S. Vogt, P. Mason, M.E. Morales-Arteaga, U.I. Narayanan, Uranium assay determination using Davies and Gray titration: an overview and implementation of GUM for uncertainty evaluation. J. Radioanal Nucl Chem 282 (2009) **939-944**.

[40] ASTM C1267-06. Standard Test Method for Uranium by Iron (II) Reduction in Phosphoric Acid Followed by Chromium (VI) Titration in the Presence of Vanadium.. 46 (2007) 11335-11344.

[41] I. May, S.D. Reilly, L.M. Colletti, Uranium concentration measurement technique viability analysis, Los Alamos National Laboratory, **(2014)** LA-UR-14-29709.

[42] M. Balcerzak, Analytical Methods for the Determination of Ruthenium: The State of the Art, Critical Reviews in Analytical Chemistry, 32 (2002), 181-226.

[43] V.M. Vdovenko, L.N. Lazarev, Ya. S. Khvorostin, Investigation of Ru(IV) solutions in perchloric and sulfuric acid, **Radiokhimiya** 7 (1964), 232-240.

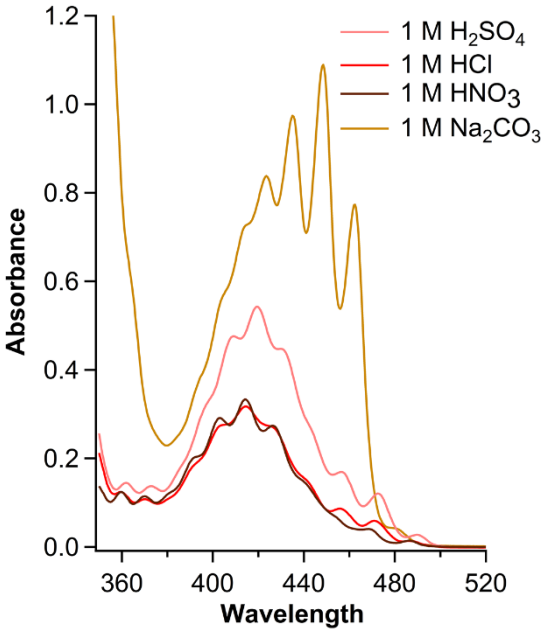

Figure 1. Absorption spectra of 8.8 mg/g uranyl(VI) in various aqueous matrices, as recorded in Starna cell 1 at 22.5 °C.

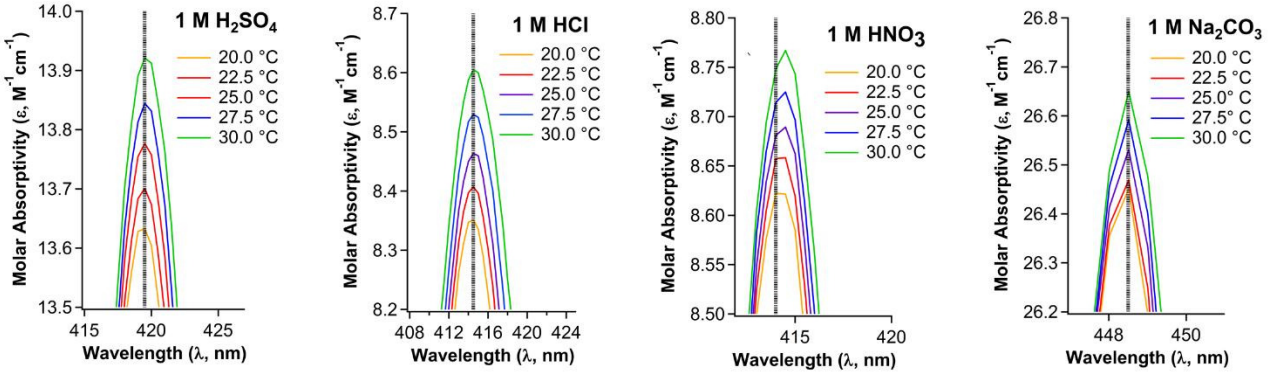

Figure 2. Spectra (Starna cell 1) shown uranyl molar absorptivity at λ_{max} in various aqueous media as a function of temperature, with the dotted line defining the wave length value used for the associated 'reads' spectroscopic data method.

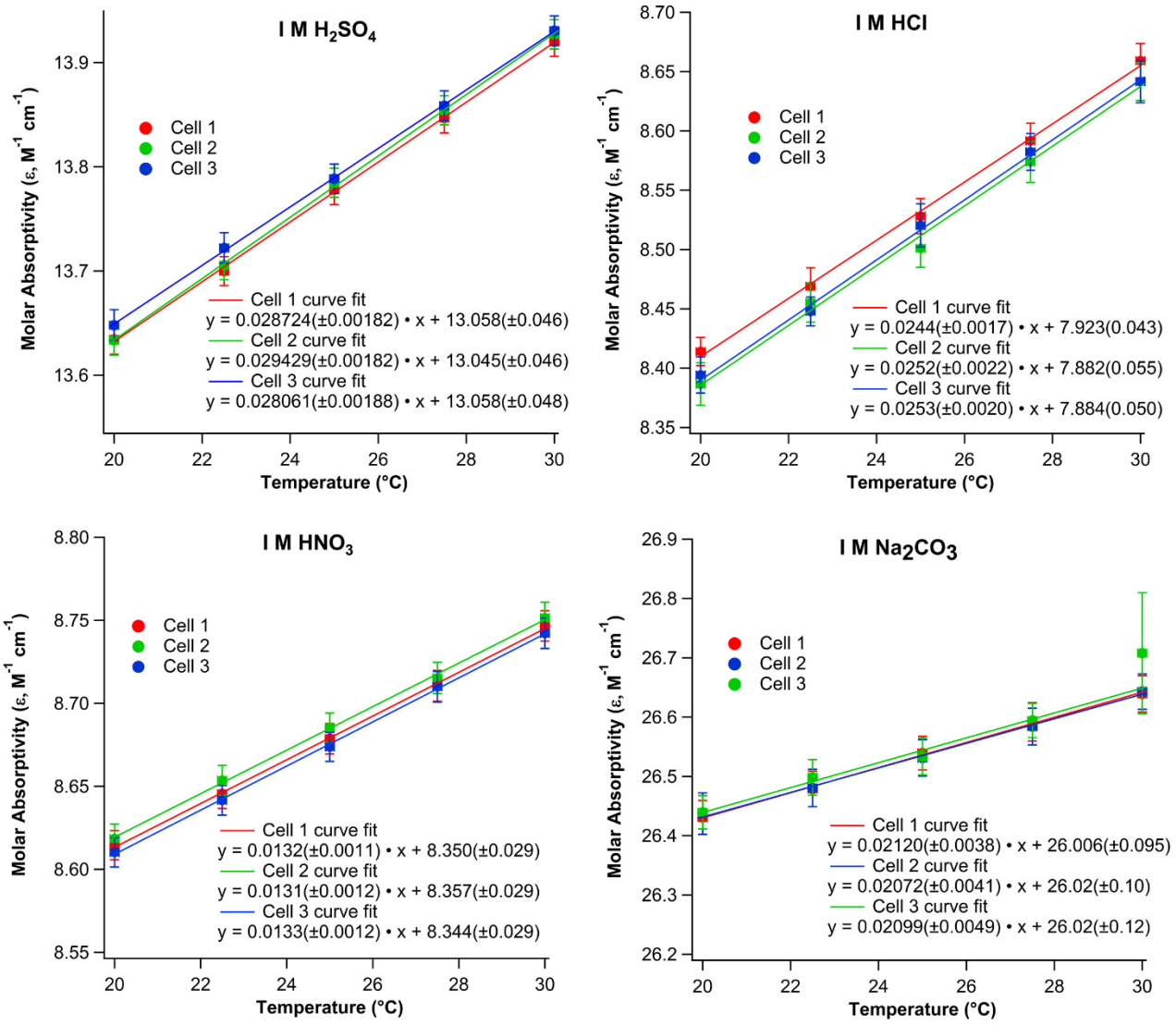

Figure 3. Calculated molar absorptivity values at λ_{max} for the uranyl cation in the visible region of the absorption spectra in 1 M H_2SO_4, HCl, HNO_3 & Na_2CO_3. The data was collected in 3 different Starna cells at 20.0, 22.5. 25.0, 27.5 & 30.0 °C, with data fits weighted to the 1σ uncertainty in both molar absorptivity and temperature.

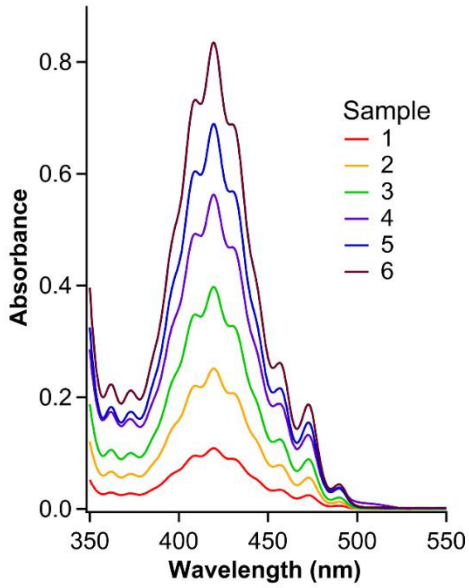

Figure 4. Visible spectra for samples 1-6 at 22.5 °C (Starna cell 1) recorded using the regular scan method.

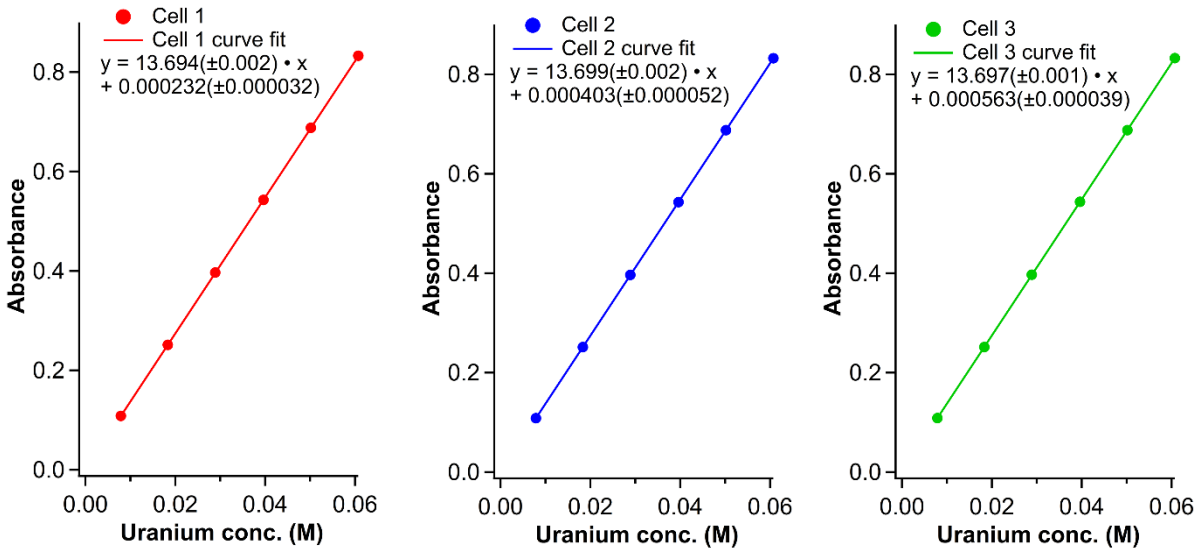

Figure 5. Plots of absorbance at λ_{max} 419.5 nm vs. uranium concentration for solutions 1-6 in 1 M H_2SO_4. The data was collected in 3 different Starna cells at 22.5 °C, with fits weighted to the 1σ uncertainty in both absorbance and uranium concentration.

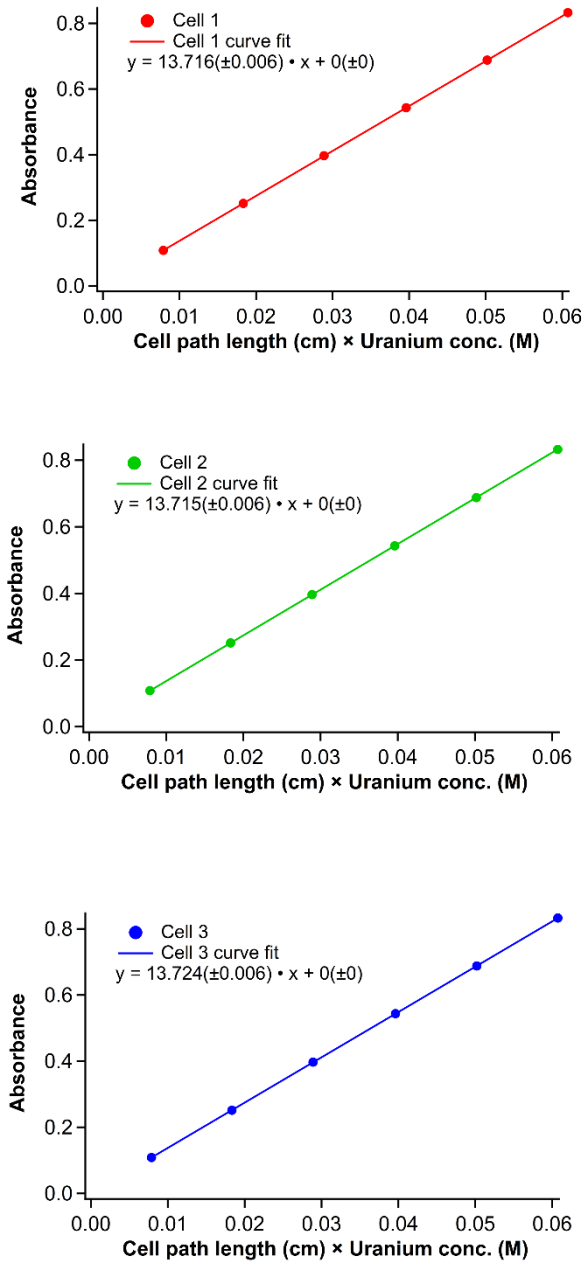

Figure 6. Plots of absorbance at λ_{max} 419.5 nm vs. uranium concentration × cell path length for solutions 1-6 in 1 M H_2SO_4. The data was collected in 3 different Starna cells at 22.5 °C, with fits weighted to the 1σ uncertainty in both absorbance and uranium concentration × cell path length, and the x & y intercepts set to 0.

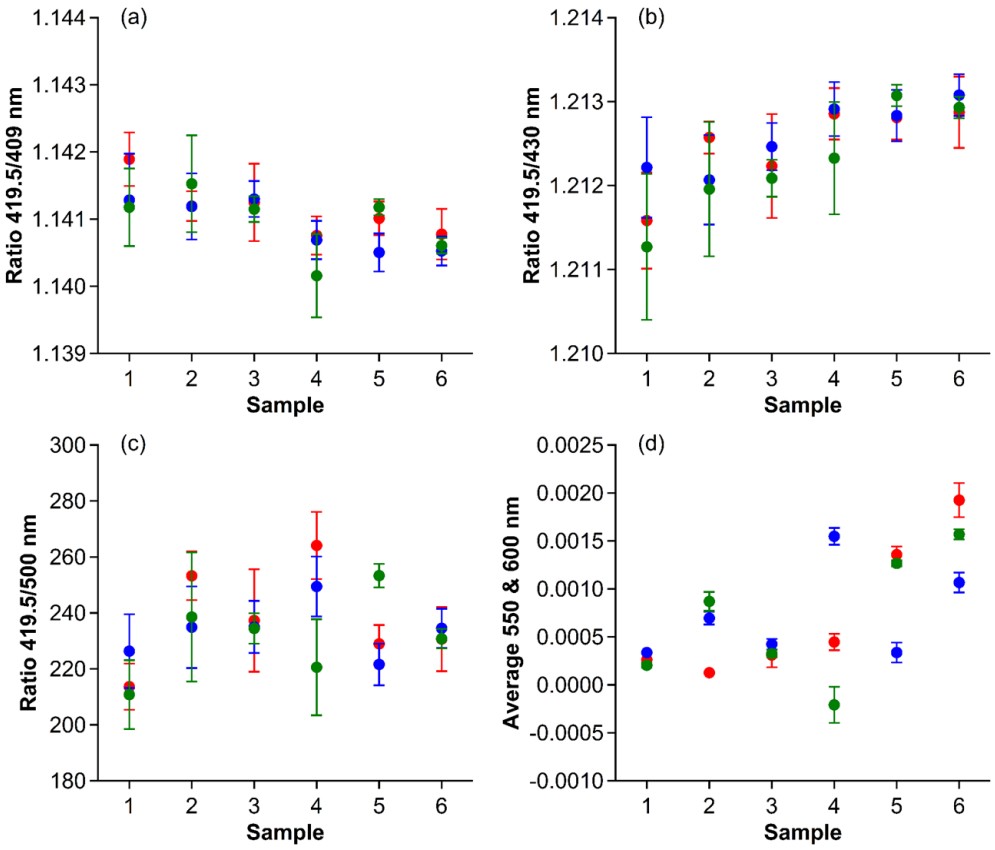

Figure 7. Analysis of absorbance values for samples 1-6 generated using the reads method for Starna Cells 1 (red), 2 (blue) and 3 (green). (a) Ratio of the 419.5/409 nm absorbance, (b) Ratio of the 419.5/430 nm absorbance, (c) Ratio of the 419.5/500 nm absorbance and (d) Average of the 550 and 600 nm absorbance. The error bars are at the 1σ uncertainty level.

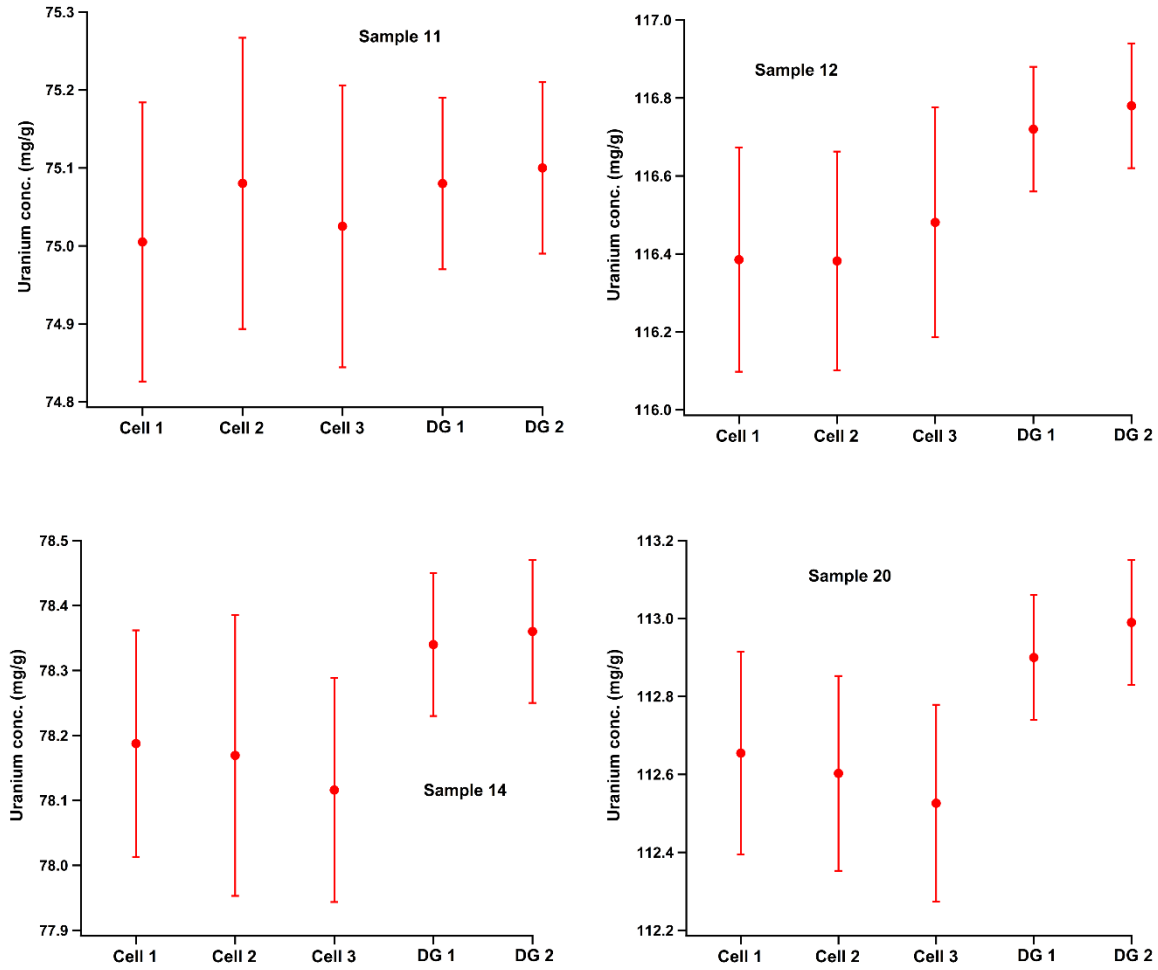

Figure 8. A comparison of uranium concentration measurements using the visible spectroscopy technique (cells 1-3) and duplicate Davies-Gray titration analysis (DG 1 and DG 2) for unknown samples 11-12, 14 & 20. Uncertainties for the spectroscopy measurements are shown at 2σ, while uncertainties for the DG measurements are reports as 0.14 %, the expected international target value (ITV).

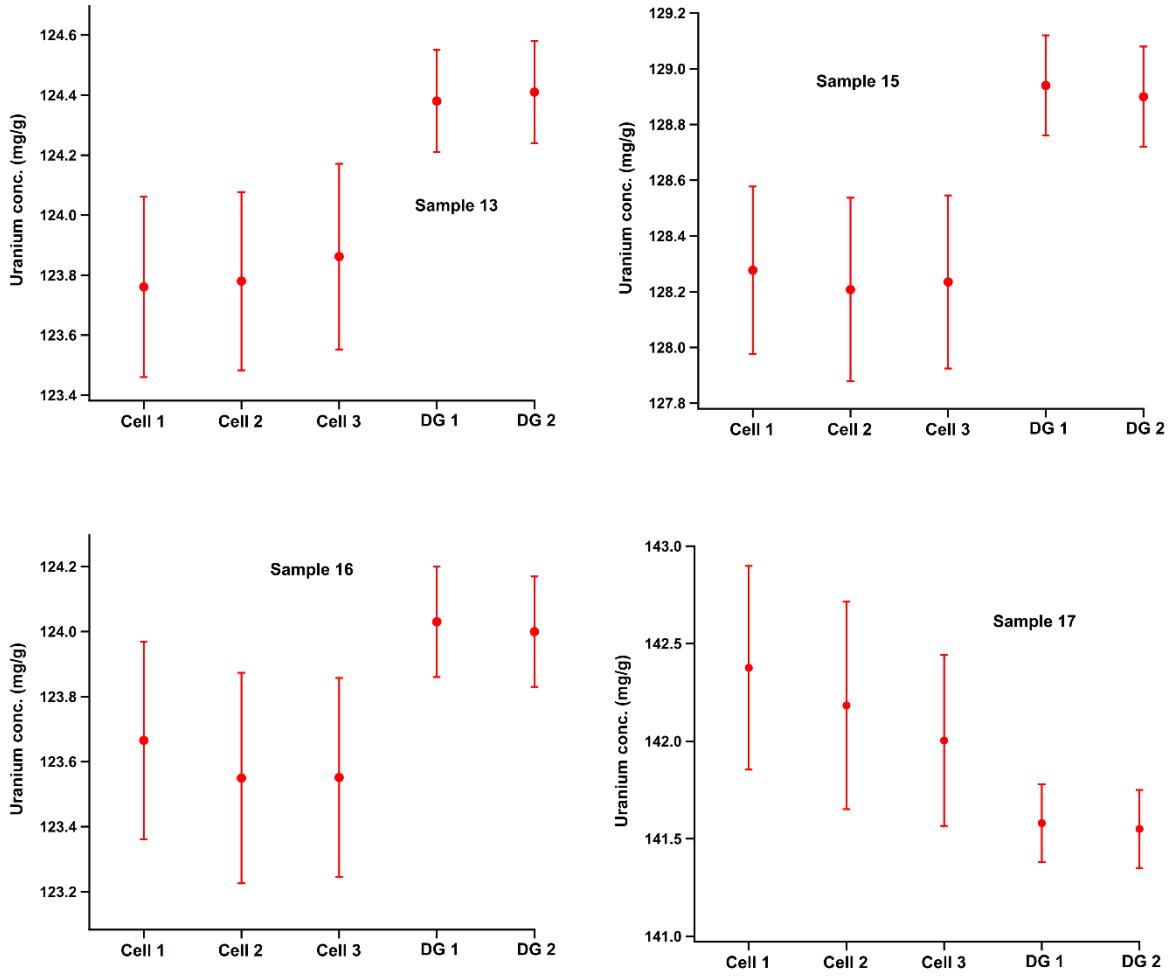

Figure 9. A comparison of uranium concentration measurements using the visible spectroscopy technique (cells 1-3) and duplicate Davies-Gray titration analysis (DG 1 and DG 2) for unknown samples 13, 15, 16-17. Uncertainties for the spectroscopy measurements are shown at 2σ, while uncertainties for the DG measurements are reports as 0.14 %, the expected international target value (ITV).

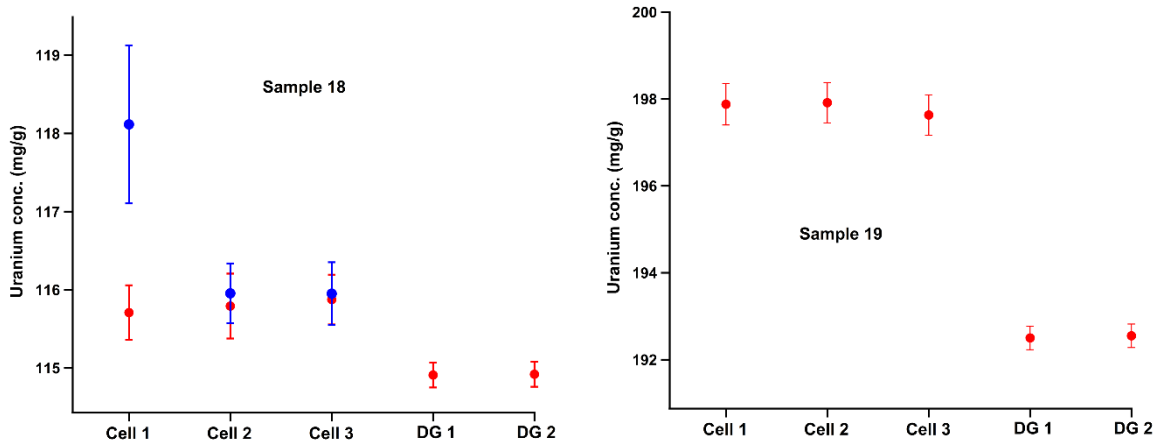

Figure 10. A comparison of uranium concentration measurements using the visible spectroscopy technique (cells 1-3) and duplicate Davies-Gray titration analysis (DG 1 and DG 2) for unknown samples 18 & 19. Repeat measurements using LabChem sulfuric acid for preparation of the assay samples for 18 (18*) are shown in blue. Uncertainties for the spectroscopy measurements are shown at 2σ, while uncertainties for the DG measurements are reports as 0.14 %, the expected international target value (ITV).

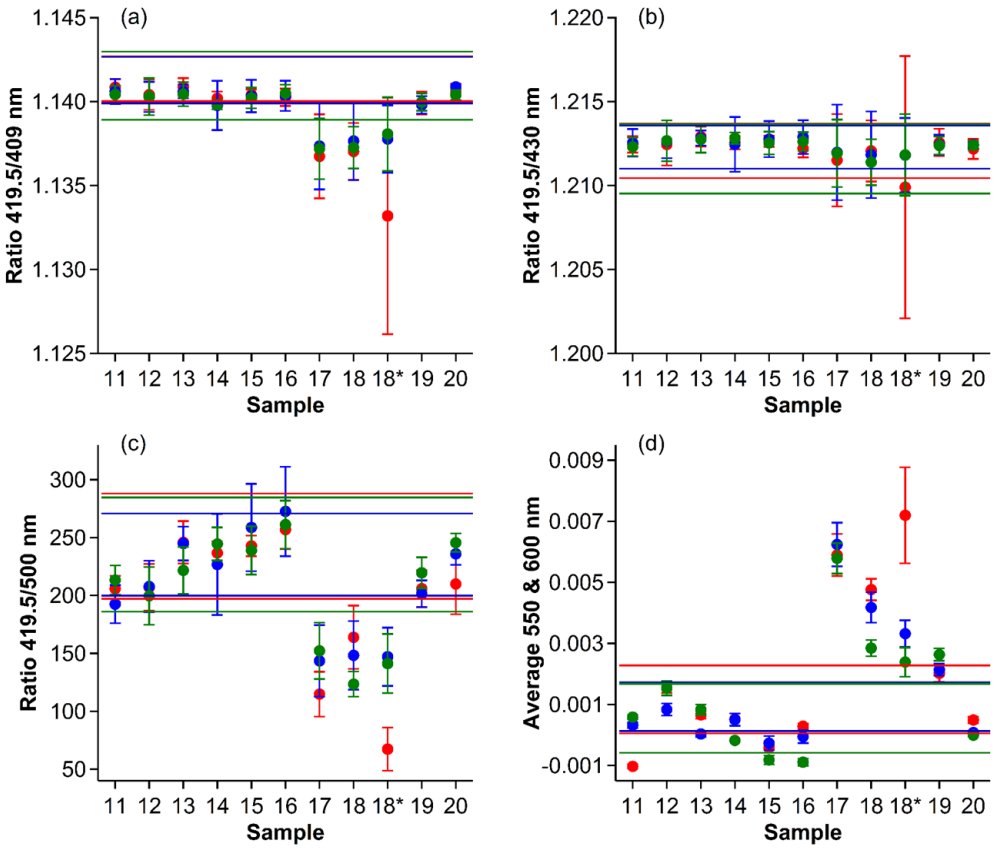

Figure 11. Analysis of absorbance values for 1 M H_2SO_4 assays of samples 11-20 generated using the reads method for Starna Cells 1 (red), 2 (blue) and 3 (green). (a) Ratio of the 419.5/409 nm absorbance, (b) Ratio of the 419.5/430 nm absorbance, (c) Ratio of the 419.5/500 nm absorbance and (d) Average of the 550 and 600 nm absorbance. The error bars are at the 1σ uncertainty level. The lines define the observed maximum (+2σ) and minimum (-2σ) values obtained from the identical analysis performed for samples 1-6 (see Figure 7).

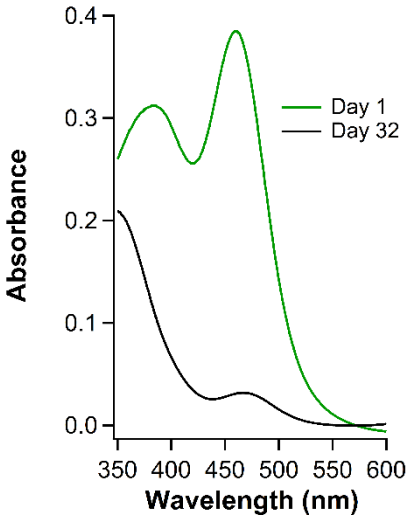

Figure 12. Absorbance spectra of 10 ppm Ru in 1 M H_2SO_4, day 1, and 32 days after sample preparation. The spectra are an average of Starna cells 1, 2 & 3, background corrected with 1 M H_2SO_4 and baseline corrected with an average absorbance of all data recorded between 550-600 nm.

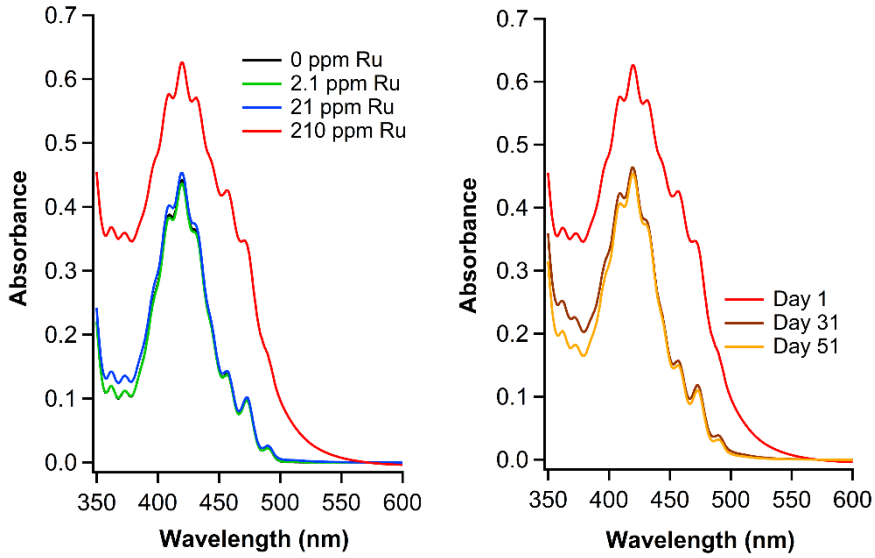

Figure 13. Absorbance spectra of 1 M H_2SO_4 assay of 129 mg/g U with **effectively** 0, 2.1, 21 & 210 ppm Ru contaminant levels (samples 21, 22, 23 & 24), recorded on day 1 (left). **In practice the Ru was initially present in the 1 MH_2SO_4 solution and thus the 210 ppm Ru contaminant level sample is actually the same as the 10 ppm Ru samples shown in Figure 12.** The 210 ppm Ru contaminant sample recorded on day 31 & 51 is also shown (right).The spectra are an average of Starna cells 1, 2 & 3, background corrected with 1 M H_2SO_4 and baseline corrected with an average absorbance of all data recorded between 550-600 nm.

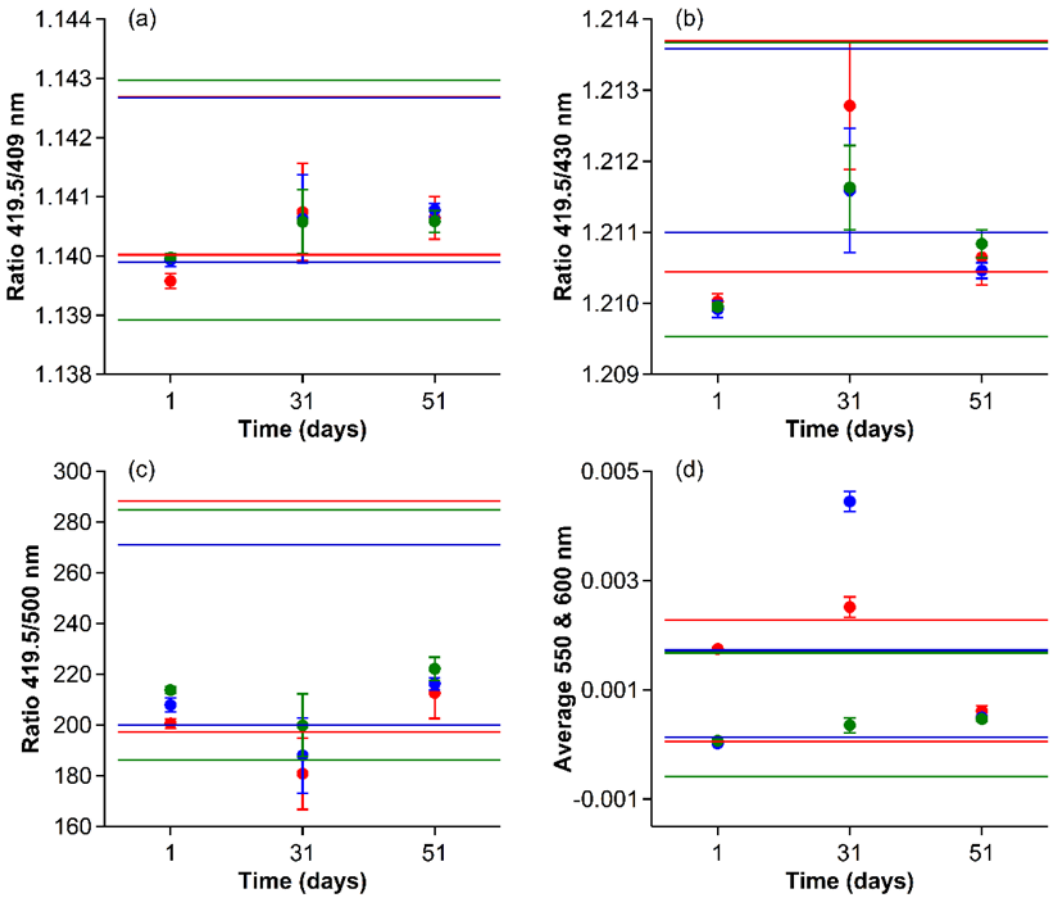

Figure 14. Analysis of absorbance values for 1 M H_2SO_4 assay of sample 21, 129 mg/g uranium and 0 ppm Ru contaminant. The measurements were recorded on day 1, day 31 & day 51, and the data generated using the reads method for Starna Cells 1 (red), 2 (blue) and 3 (green). (a) Ratio of the 419.5/409 nm absorbance, (b) Ratio of the 419.5/430 nm absorbance, (c) Ratio of the 419.5/500 nm absorbance and (d) Average of the 550 and 600 nm absorbance. The error bars are at the 1σ uncertainty level. The lines define the observed maximum (+2σ) and minimum (-2σ) values obtained from the identical analysis performed for samples 1-6.

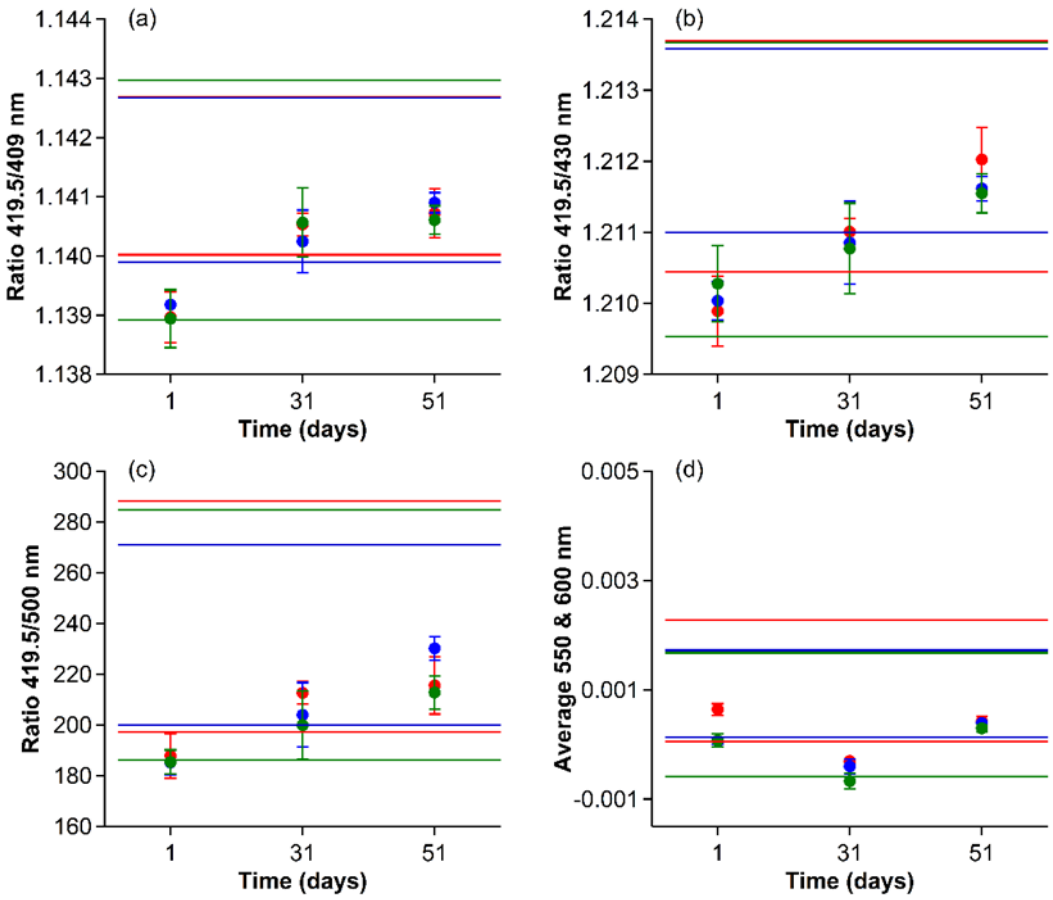

Figure 15. Analysis of absorbance values for 1 M H_2SO_4 assay of sample 22, 129 mg/g uranium and 2.1 ppm Ru contaminant. The measurements were recorded on day 1, day 31 & day 51, and the data generated using the reads method for Starna Cells 1 (red), 2 (blue) and 3 (green). (a) Ratio of the 419.5/409 nm absorbance, (b) Ratio of the 419.5/430 nm absorbance, (c) Ratio of the 419.5/500 nm absorbance and (d) Average of the 550 and 600 nm absorbance. The error bars are at the 1σ uncertainty level. The lines define the observed maximum (+2σ) and minimum (-2σ) values obtained from the identical analysis performed for samples 1-6.

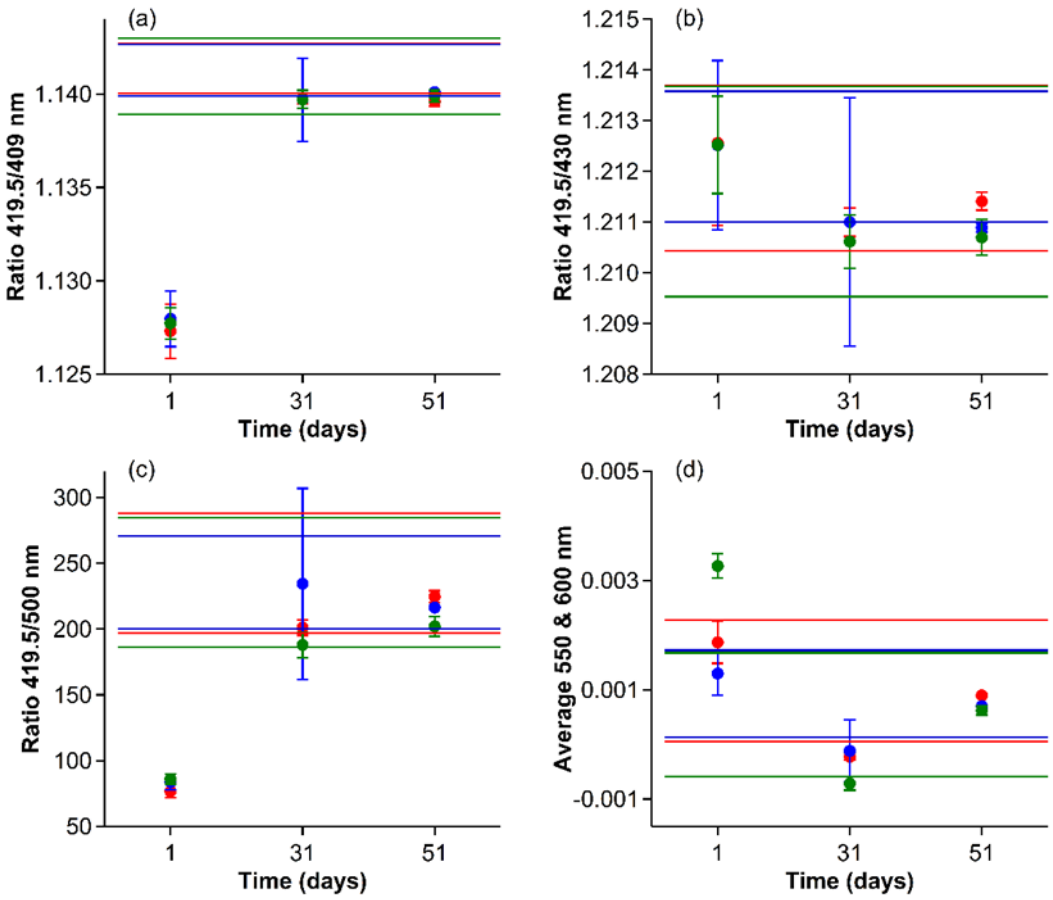

Figure 16. Analysis of absorbance values for 1 M H_2SO_4 assay of sample 23, 129 mg/g uranium and 21 ppm Ru contaminant. The measurements were recorded on day 1, day 31 & day 51, and the data generated using the reads method for Starna Cells 1 (red), 2 (blue) and 3 (green). (a) Ratio of the 419.5/409 nm absorbance, (b) Ratio of the 419.5/430 nm absorbance, (c) Ratio of the 419.5/500 nm absorbance and (d) Average of the 550 and 600 nm absorbance. The error bars are at the 1σ uncertainty level. The lines define the observed maximum (+2σ) and minimum (-2σ) values obtained from the identical analysis performed for samples 1-6.

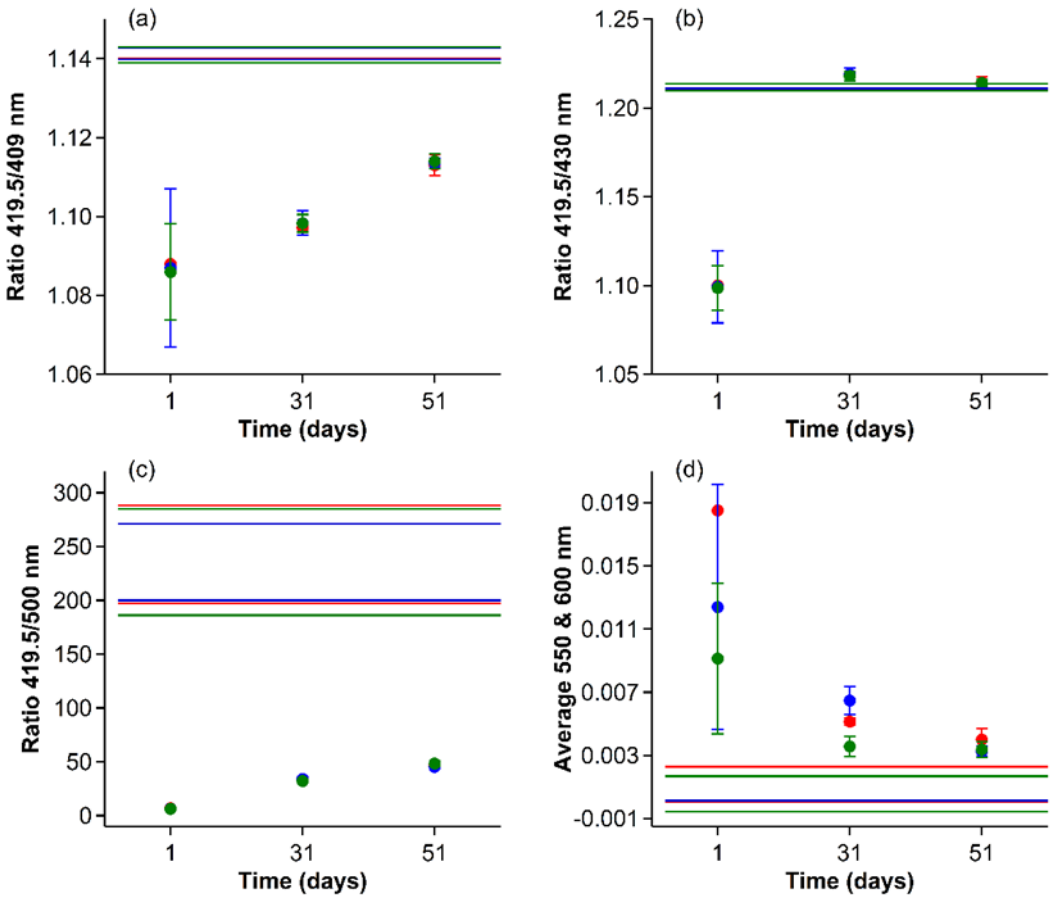

Figure 17. Analysis of absorbance values for 1 M H_2SO_4 assay of sample 24, 129 mg/g uranium and 210 ppm Ru contaminant. The measurements were recorded on day 1, day 31 & day 51, and the data generated using the reads method for Starna Cells 1 (red), 2 (blue) and 3 (green). (a) Ratio of the 419.5/409 nm absorbance, (b) Ratio of the 419.5/430 nm absorbance, (c) Ratio of the 419.5/500 nm absorbance and (d) Average of the 550 and 600 nm absorbance. The error bars are at the 1σ uncertainty level. The lines define the observed maximum (+2σ) and minimum (-2σ) values obtained from the identical analysis performed for samples 1-6.

Equation 1. Determination of molar absorptivity ε (cm^{-1} M^{-1}) at λ_{max}.

$$\boldsymbol{\varepsilon} = \frac{\boldsymbol{a}}{\boldsymbol{b} \cdot \boldsymbol{c}}$$

$$\boldsymbol{\sigma_\varepsilon} = \sqrt{\left(\frac{\mathbf{1}}{\boldsymbol{b} \cdot \boldsymbol{c}}\right)^2 \cdot \boldsymbol{\sigma_a}^2 + \left(-\frac{\boldsymbol{a}}{\boldsymbol{b}^2 \cdot \boldsymbol{c}}\right)^2 \cdot \boldsymbol{\sigma_b}^2 + \left(-\frac{\boldsymbol{a}}{\boldsymbol{b} \cdot \boldsymbol{c}^2}\right)^2 \cdot \boldsymbol{\sigma_c}^2}$$

Where: $\boldsymbol{a}$ = baseline and background corrected UV-vis absorbance at λ_{max}.

$\boldsymbol{b}$ = UV-vis cuvette path length (cm) = 1.000 ± 0.001 cm.

$\boldsymbol{c}$ = Uranium concentration (mol U/L) at the measurement temperature.

Equation 2. Determination of molar uranium concentration, [U].

$$[U] = \left(\frac{\frac{x}{y} + \frac{u}{v}}{\frac{x}{y}}\right) \cdot \frac{a}{z \cdot b} = \frac{a}{z \cdot b} + \frac{a \cdot u \cdot y}{v \cdot x \cdot z \cdot b}$$

$$\sigma_{[U]} = \sqrt{\begin{array}{c}\left(-\frac{a \cdot u \cdot y}{v \cdot b \cdot x^2 \cdot z}\right)^2 \cdot \sigma_x{}^2 + \left(\frac{a \cdot u}{v \cdot b \cdot x \cdot z}\right)^2 \cdot \sigma_y{}^2 + \left(\frac{a \cdot y}{v \cdot b \cdot x \cdot z}\right)^2 \cdot \sigma_u{}^2 + \left(-\frac{a \cdot u \cdot y}{v^2 \cdot b \cdot x \cdot z}\right)^2 \cdot \sigma_v{}^2 + \\ \left(\frac{u \cdot y + v \cdot x}{v \cdot b \cdot x \cdot z}\right)^2 \cdot \sigma_a{}^2 + \left(-\frac{a \cdot (u \cdot y + v \cdot x)}{v \cdot b \cdot x \cdot z^2}\right)^2 \cdot \sigma_z{}^2 + \left(-\frac{a \cdot (u \cdot y + v \cdot x)}{v \cdot b^2 \cdot x \cdot z}\right)^2 \cdot \sigma_b{}^2\end{array}}$$

Where: $\boldsymbol{x}$ = uranium sulfate solution aliquot mass (g)

$\boldsymbol{y}$ = measured neat uranium sulfate solution density (g/mL)

$\boldsymbol{u}$ = 1.0 M H_2SO_4 solution mass (g)

$\boldsymbol{v}$ = measured 1.0 M H_2SO_4 density (g/mL)

$\boldsymbol{a}$ = measured background and baseline corrected absorbance at λ_{max}.

$\boldsymbol{b}$ = UV-vis cuvette path length (cm) = 1.000 ± 0.001 cm

$\boldsymbol{z}$ = ε at λ_{max} (M^{-1} cm^{-1})

Equation 3. Determination of mg/g uranium concentration

$$[U](mg/g) = \frac{x \cdot z}{10^3 \cdot y}$$

$$\sigma_{[U](mg/g)} = \sqrt{\left(\frac{z}{10^3 \cdot y}\right)^2 \cdot \sigma_x{}^2 + \left(\frac{x}{10^3 \cdot y}\right)^2 \cdot \sigma_z{}^2 + \left(-\frac{x \cdot z}{10^3 \cdot y^2}\right)^2 \cdot \sigma_y{}^2}$$

Where: $\boldsymbol{x}$ = molar uranium concentration, as calculated in Eqn. 2. (mol U/L solution)

$\boldsymbol{y}$ = uranium sulfate solution density (g/mL) at UV-vis data collection temperature

$\boldsymbol{z}$ = molecular weight (g/mol) of U in standard natural uranium samples (238.02892±0.00012) or depleted uranium samples (238.042±0.010)

Table 1. Solutions 1-9, aqueous solution matrix and uranium concentration (1σ uncertainty).

Soln. No.	Matrix (1 M)	[U] (mg/g)	[U] (mM) at 22.5 °C
1	H_2SO_4	1.76747(±0.00022)	7.8826(±0.0010)
2	H_2SO_4	4.10160(±0.00030)	18.3404(±0.0015)
3	H_2SO_4	6.44515(±0.00045)	28.8932(±0.0023)
4	H_2SO_4	8.81531(±0.00059)	39.6182(±0.0023)
5	H_2SO_4	11.13931(±0.00037)	50.1924(±0.0025)
6	H_2SO_4	13.44797(±0.00083)	60.7390(±0.0044)
7	HCl	8.76573(±0.00056)	37.7444(±0.0028)
8	HNO_3	8.79585(±0.00055)	38.4583(±0.0028)
9	Na_2CO_3	8.84495(±0.00058)	41.1519(±0.0033)

Table 2. Molar absorptivity (ε, M^{-1} cm^{-1}) at λ_{max} for uranyl(VI) in 1 M aqueous solutions at various temperatures. All measurements were made in 3 different 10 mm path length Starna cells, with uncertainties reported to 1σ.

Temp.	Cell No.	1 M H_2SO_4 (λ_{max} 419.5 nm)	1 M HCl (λ_{max} 414.5 nm)	1 M HNO_3 (λ_{max} 414.0 nm)	1 M Na_2CO_3 (λ_{max} 448.5 nm)
20.0 °C	1	13.634(±0.014)	8.414(±0.012)	8.615(±0.009)	26.431(±0.029)
20.0 °C	2	13.634(±0.014)	8.387(±0.018)	8.619(±0.009)	26.437(±0.035)
20.0 °C	3	13.648(±0.015)	8.394(±0.015)	8.610(±0.009)	26.440(±0.028)
22.5 °C	1	13.700(±0.014)	8.469(±0.016)	8.646(±0.009)	26.479(±0.030)
22.5 °C	2	13.706(±0.014)	8.455(±0.016)	8.654(±0.009)	26.481(±0.032)
22.5 °C	3	13.722(±0.015)	8.448(±0.012)	8.642(±0.009)	26.498(±0.030)
25.0 °C	1	13.778(±0.014)	8.528(±0.015)	8.679(±0.009)	26.539(±0.028)
25.0 °C	2	13.785(±0.014)	8.501(±0.016)	8.685(±0.009)	26.531(±0.031)
25.0 °C	3	13.789(±0.014)	8.520(±0.018)	8.674(±0.009)	26.533(±0.031)
27.5 °C	1	13.847(±0.014)	8.592(±0.015)	8.711(±0.009)	26.592(±0.032)
27.5 °C	2	13.854(±0.014)	8.574(±0.017)	8.715(±0.009)	26.584(±0.031)
27.5 °C	3	13.859(±0.014)	8.582(±0.016)	8.710(±0.009)	26.594(±0.029)
30.0 °C	1	13.920(±0.014)	8.659(±0.014)	8.747(±0.009)	26.639(±0.031)
30.0 °C	2	13.927(±0.014)	8.641(±0.016)	8.752(±0.009)	26.643(±0.030)
30.0 °C	3	13.931(±0.014)	8.641(±0.018)	8.742(±0.009)	26.708(±0.102)

Table 3. Molar absorptivity values (ε, M^{-1} cm^{-1}) calculated individually at λ_{max} (419.5 nm) for uranium samples 1 – 6 (1 M H_2SO_4) in the three different 1 cm Starna cells (22.5 °C).

Starna Cell	Sample 1	Sample 2	Sample 3	Sample 4	Sample 5	Sample 6
1	13.749(±0.014)	13.701(±0.014)	13.733(±0.014)	13.700(±0.014)	13.705(±0.014)	13.710(±0.014)
2	13.744(±0.015)	13.711(±0.014)	13.725(±0.014)	13.706(±0.014)	13.704(±0.014)	13.704(±0.014)
3	13.760(±0.015)	13.711(±0.014)	13.741(±0.014)	13.722(±0.015)	13.701(±0.014)	13.709(±0.014)

Table 4. Absorbance values recorded in the three different 10 mm Starna cells at the different uranium molar concentrations (samples 1-6) at 22.5 °C, and the contribution of cell path length - required to generate the molar absorptivity values across the concentration range (Figure 6.)

Sam	Cell 1	Cell 2	Cell 3	[Uranium] (M)	Cell path length (cm) ×
1	0.10838(±0.0	0.10834(±0.0	0.10846(±0.0	0.007883(±0.00	0.00788(±0.00001)
2	0.25128(±0.0	0.25146(±0.0	0.25147(±0.0	0.01834(±0.000	0.01834(±0.00002)
3	0.39680(±0.0	0.39656(±0.0	0.39703(±0.0	0.028893(±0.00	0.02889(±0.00003)
4	0.54276(±0.0	0.54299(±0.0	0.54365(±0.0	0.039618(±0.00	0.03962(±0.00004)
5	0.68790(±0.0	0.68784(±0.0	0.68771(±0.0	0.050192(±0.00	0.05019(±0.00005)
6	0.83275(±0.0	0.83235(±0.0	0.83268(±0.0	0.060739(±0.00	0.06074(±0.00006)

Table 5. Uranium concentration measurements for samples 11-20, as determined by both visible spectroscopy and Davies-Gray titration analysis. Sample 18 was analyzed spectroscopically through assay into 1 M H_2SO_4 prepared from both Fisher and LabChem (*) 2 M H_2SO_4. Spectroscopic data are reported from analysis in 3 different 10.0 mm Starna cells, with expanded (2σ) uncertainties. Davies and Gray uncertainties are reported with uncertainties equivalent to the 0.14 % International Target Value (ITV), with relative standard deviation between the duplicate analyses all being less than this value.

Sample	Visible Spectroscopy			Davies-Gray	
	Cell 1	Cell 2	Cell 3	Duplicate Measurements	
11	75.01(±0.18)	75.08(±0.19)	75.03(±0.18)	75.08(±0.11)	75.10(±0.11)
12	116.39(±0.29)	116.38(±0.28)	116.48(±0.30)	116.72(±0.16)	116.78(±0.16)
13	123.76(±0.30)	123.78(±0.30)	123.86(±0.31)	124.38(±0.17)	124.41(±0.17)
14	78.19(±0.17)	78.17(±0.22)	78.12(±0.17)	78.34(±0.11)	78.36(±0.11)
15	128.28(±0.30)	128.21(±0.33)	128.23(±0.31)	128.94(±0.18)	128.90(±0.18)
16	123.67(±0.30)	123.55(±0.32)	123.55(±0.31)	124.03(±0.17)	124.00(±0.17)
17	142.38(±0.52)	142.18(±0.53)	142.00(±0.44)	141.58(±0.20)	141.55(±0.20)
18	115.71(±0.35)	115.79(±0.41)	115.88(±0.32)	114.91(±0.16)	114.92(±0.16)
18*	118.12(±1.01)	115.96(±0.38)	115.95(±0.40)	114.91(±0.16)	114.92(±0.16)
19	197.88(±0.48)	197.91(±0.46)	197.63(±0.46)	192.50(±0.27)	192.55(±0.27)
20	112.65(±0.26)	112.60(±0.25)	112.53(±0.25)	112.90(±0.16)	112.99(±0.16)

Table 6. Measured [U] (mg/g) in samples 21-24, that were spiked with Ru contaminant, using the visible spectroscopy assay into 1 M H_2SO_4 technique. The samples were analyzed after the initial sample preparation and then 31 and 51 days later. The temperature was not controlled during the sample analysis and thus temperature dependent molar absorptivity values were used to calculate [U]. For Starna cells 1, 2 & 3 ε ($M\ cm^{-1}$) was **13.368 + (0.019×T), 13.450 + (0.017×T) & 13.443 + (0.017×T)**, respectively (where T = measurement temperature, °C). Uncertainties are reported to 2σ.

Sample	Day 1 [U] mg/g			Day 31 [U] mg/g			Day 51 [U] mg/g		
(Ru ppm)	Cell 1	Cell 2	Cell 3	Cell 1	Cell 2	Cell 3	Cell 1	Cell 2	Cell 3
21 (0)	129.43	129.12	129.44	129.46	129.03	128.99	129.37	129.18	129.22
	(±1.02)	(±0.99)	(±1.03)	(±0.97)	(±0.95)	(±0.98)	(±0.98)	(±0.95)	(±0.98)
22 (2.1)	129.67	129.59	129.71	129.81	129.62	129.69	129.69	129.46	129.60
	(±1.03)	(±1.00)	(±1.03)	(±1.00)	(±0.97)	(±1.01)	(±0.97)	(±0.95)	(±0.99)
23 (21)	132.50	132.24	131.85	129.46	129.20	129.46	129.31	129.22	129.35
	(±1.07)	(±1.04)	(±1.06)	(±1.01)	(±1.03)	(±1.01)	(±1.01)	(±0.98)	(±1.02)
24 (210)	184.58	185.83	187.17	138.32	138.20	138.51	135.39	135.29	135.24
	(±1.46)	(±4.84)	(±3.22)	(±1.09)	(±1.17)	(±1.15)	(±1.14)	(±1.05)	(±1.01)

Highlights:

- A visible absorption spectroscopy uranium analysis technique.
- Uranium analysis to within 0.3 % of results obtained by Davies-Gray analysis.
- Technique sensitive to impurities.